Low frequency, low level ranging method for the broadband access facilities network of RACE 2024

van Oyen, A.L.C.

Award date:
1993

Low frequency, low level ranging method

for the Broadband Access Facilities
network of RACE 2024

by A.L.C. van Oyen

Report of the graduation project,
carried out from january 1993 till september 1993

Supervisors: ir. T.W.M. Mosch (AT&T)
prof. ir. M.P.J. Stevens (TUE)

Preface

This report is a reflection of my study activities for my graduation project concerning a new ranging method for a broadband access facilities network. But to graduate is much more than only study activities. Just the mixture of study and all those other things made my graduation period at AT&T as an instructive, interesting and very pleasant experience. That is why I would like to thank the people who made this all possible. Especially I would like to thank the members of the U-team and my supervisor ir. Theo Mosch who were always very supportive and understanding. Also I would like to thank my parents and girlfriend for their patience and understanding during my graduation period.

Anthony van Oyen

dedicated to Toon Vugts

Summary

In RACE project 2024 a broadband access facilities network, called BAF, is under study. This network is based on ATM over a passive optical network and has a maximum splitting ratio of 32. This means that maximum 32 Network Units can be connected to a Line Termination. The distance between a Network Unit and the Line Termination is maximum 10 km. The used transfer mode for the upstream data traffic (from NU to LT) is Time Division Multiple Access. Because the Line Termination - Network Unit connections have different distances and thus different delay times, there must be taken care of that every Network Unit send its data in the appropriate timeslot. Otherwise there will occur data collisions in the network. To solve this problem a ranging procedure has been proposed which puts all Network Units at the same virtual distance. The first step of this ranging procedure is called static coarse ranging and must determine the transfer delay with an accuracy of half a timeslot. This static coarse ranging uses a low frequency, low level signal which is superimposed on the upstream data traffic by the Network Unit under ranging and is outside the relevant frequency spectrum of the data. The Line Termination detects this ranging signal and determines the phase of the received signal. The phase of the received signal is a measure for the delay time.

The ranging signal is generated digital in the Network Unit, so the start phase of the ranging signal is easy to define. The detection in the Line Termination is done by sampling in the gap between adjacent BAF-cells. The signal is not filtered before sampling to avoid data interference. Next the phase is determined by digital signal processing which uses discrete fourier transformation techniques. The advantages of the digital signal processing method are: it is very flexible, achieves a high precision and the influence of higher harmonics is negligible. A disadvantage is the required CPU-time. Other advantages of the low frequency, low level ranging method are: the data traffic of other Network Units is not interrupted, the measurement is not influenced by the data traffic and the ranging signal can be used for other purposes like fibre monitoring. The extra amount of light received by the Line Termination is a disadvantage.

The static coarse ranging path has been considered and there has been made a description of the error sources which are divided in static errors and dynamic errors. The performance of the static coarse ranging has been calculated and has been compared with the results of the simulation program SIM, which has been developed to simulate the static coarse ranging. There has been found a close agreement between the simulation results and the calculated performance.

The proposed static coarse ranging configuration with an A/D converter of 12 bits, a measurement over 15 periods and the digital signal processing method which uses 5 samples per period for the DFT fulfills the requirements and in worst case 0.30% of the static coarse ranging procedures fails.

To improve the accuracy of the static coarse ranging the number of periods which is used for the phase measurement must be increased. The maximum feasible accuracy is determined by the static error sources and in our case this is 11.2 bits.

Contents

1. Introduction

To gain the grade of Electrical Engineer you have to finish your study program at the university with a graduation project of at least six months. I fulfilled this graduation project at the department Explorations of the AT&T NS-NL telecommunications company in Huizen.
The Explorations department operates in the field of the advanced development of public telecommunication network products. A close cooperation exists between Explorations and the AT&T Bell Labs in America. Currently the Explorations department is studying several subjects, most of which are tied to the European RACE program. For example HDWDM for the local loop (multi-wavelength system for interactive broadband traffic), RACE 2062 (components for fibre to the home), RACE 1051 (multi-gigabit project) and RACE 2024 (Broadband Access Facilities). I joined the Broadband Access Facilities (RACE 2024) project from january till september 1993.
At the moment the Broadband Access Facilities project is one of the largest projects of the department. The entire project consists of 16 partners and costs 162 staffyears over 3 years. AT&T is the prime contractor of this project and contributes 36 staffyears. The general objective of this project is to enhance the common understanding and the knowledge on Broadband Access Facilities (on the conceptual, technical and application level) for small business and residential subscribers, to enable the timely introduction of broadband services throughout the European Community. More specific objectives of the project are

- to provide guidelines for technical and economical applicability of Access Systems oriented toward broadband network applications,
- to carry out a study activity on general aspects of broadband access topics,
- to implement a lab demonstrator (622 Mbit/s, ATM on PON).

To achieve these objectives the structure of the project is as follows: in the first year (1992) the project started with general study and specification of the demonstrator, in the second year (1993) the activities concentrate on development and realization and in the final year (1994) the demonstrator system will be tested and experiments will be performed.
In the BAF network ATM over a Passive Optical Network (APON) is used. Downstream, from Line Termination to Network Termination, we have a continuous cell based traffic flow based on broadcast with selection, so extra attention has to be paid to the security of the data. The transfer mode which is used upstream, is Time Division Multiple Access. In the BAF network there are different LT-NT distances (max. 10 km) and thus different delay times. When TDMA is used a NT must put its data in an allocated timeslot, so all NT's must be synchronized to avoid collisions of data packets of NT's with different delay times. A ranging procedure is proposed to solve this problem by measuring the delay time between LT and NT and to adjust an electronic delay line in the NT. The result is that all NT's are put at the same virtual distance.
This ranging procedure consists of three parts: static coarse, static fine and dynamic fine ranging. The first part, static coarse ranging, has to make a rough estimation of the delay between LT and NT. For this static coarse ranging a new method has been proposed which is based on the phase-measurement of a low frequency, low level signal superimposed on the upstream data.

The graduation project was to study the concept and the inaccuracy of this low frequency, low level ranging method and to verify the results of these studies with a simulation program.
The report is organized as follows: in chapter 2 a brief description of the BAF project. In chapter 3 the purpose of ranging and the principle operation of static coarse ranging are explained and in chapter 4 the concept of the Static Coarse Ranging is given. The error sources and the feasible accuracy are discussed in chapter 5 and 6. A description of the simulation program and its results are given in chapter 7. Finally conclusions and recommendations are given in chapter 8.

2. The Broadband Access Facilities project

ATM broadband access is one of the subjects, which are under study at the department Explorations. The ATM broadband access is studied in the BAF project. The project is about the provision of broadband interactive services in the local loop, using ATM.
In this project, which is conducted in the framework of the European RACE II program 16 partners and associated partners are participating. The project has the following objectives:

- to enhance knowledge on Broadband Access Facilities for residential and small business subscribers,
- to provide guidelines for technical and economical applicability of Access Systems oriented toward broadband network applications,
- to carry out a study activity on general aspects of broadband access topics,
- to implement a lab demonstrator (622 Mbit/s, ATM on PON),
- to provide BAF to existing field trial (early 1995, outside project).

The main characteristics of the system defined in the BAF project are:

- Tree and Branch PON topology, splitting ratio of 32
- 622 Mbit/s up- and downstream bitrate
- 30 dB power budget required, 1300 nm window
- ATM single cell based transmission
- WDM's included for use of 1550 nm window
- maximum distance 10 km

In figure 2.1 the general architecture of the BAF network is depicted. The BAF system is an access system for the small and residential customers with a maximum number of 81 Broadband interfaces.The system consists of network, user and management components

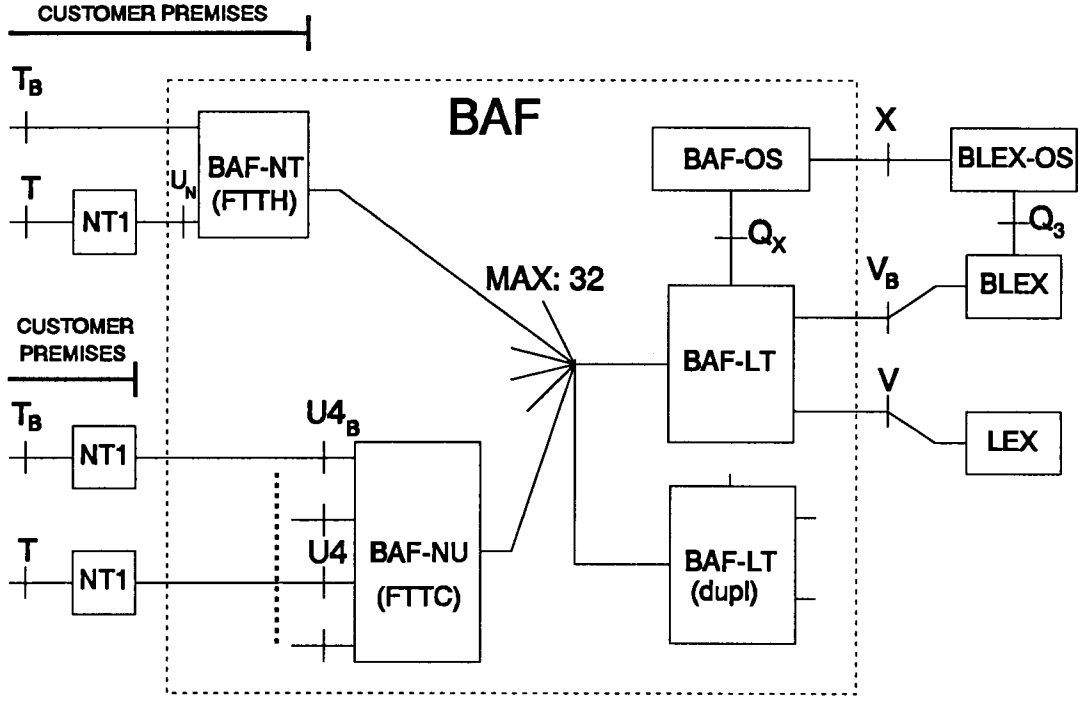

figure 2.1: General architecture BAF-network

First the BAF Line Termination (LT), this is the unit located at the network end of the system and contains the standardized V_B-interfaces (4*155 Mb/s, Synchronous Transfer Mode (STM)) to the network (LEX / X connect), the U-interface (622 Mb/s interface) to the Branching network and the Qx-management interface to the BAF Operating System.
Second the BAF Network Unit/Termination (NU, NT), this is the interface to the customer premises. The NT is intended for individual customers with up to a 155 Mb/s bandwidth requirement (Fibre To The Home, FTTH). It therefore has only one T_B-interface at the STM1 rate. It interfaces to the Branching network at 622 Mb/s over the U-interface. The NU is shared resource with up to 10 customers sharing the same unit (Fibre To The Curb, FTTC). Each customer has the ability to use up to 155 Mb/s of bandwidth (STM1, T-interfaces) with a total capacity of 622 Mb/s shared between them.
Next the BAF Branching network (BRAN), up to 32 NT's (or NU's, or a mixture of the two) may share the same fibre using Time Division Multiple Access (TDMA) techniques for upstream traffic. System cost reduction is achieved by sharing the costs of the Line Termination. The maximum distance between the customer and the Line Termination is 10 km.
Finally we have the BAF Operating System (OS). The management of the system is controlled from a workstation and interfaces to the BAF network over the Qx interface. This is done via the control card located in the Line Termination equipment. The Operating System interfaces to the LCRF_OS (Management Simulator) via the X Management interface. The OS allows the BAF network parameters to be configured. It takes action when problems are detected in the network or its performance degrades. The OS provides a graphical user interface.

This architecture results in the following external interfaces:

Customer side:		
- Broadband:	T_B, $U4_B$	(I.432 , 155 Mb/s, ATM in STM1)
- Narrowband:	U_N	(G.703 , 2 Mb/s unrestricted)
Network side:		
- Broadband:	V_B	(.... , 622 Mb/s, ATM in STM4)
- Narrowband:	V	(G.703 , 2 Mb/s unrestricted)

In the BAF network two different transfer modes are used. First downstream we have broadcast with selection. All the NT's receive all the downstream data and the NT has to pick out his own data. Because all the NT's receive the same data, the security in the network is a major aspect.
The used transfer mode for the upstream traffic is Time Division Multiple Access (TDMA) and the distance between the Line Termination (LT) and the Network Termination/Unit (NT/NU) is maximum 10 km. If we do not know the network delay then collisions in the network will occur due to different fibre delays in the data path according to different LT - NU connections, so it is necessary to determine the network delay between NU and LT. Therefore a so called ranging procedure is introduced. The ranging procedure consists of three parts: static coarse, static fine and dynamic fine ranging. The first part, static coarse ranging, must determine the physical delay.
A simple solution to this problem is to order all NU's to remain silent and send a command to the NU under ranging and wait for his response. This method however has some serious drawbacks. For example the time to wait for response has to be the maximum round-trip time, the transmission capacity decreases and a number of cells have

to be buffered at the NT-side. To overcome this a new out-of-band method has been proposed. This ranging method is based on the phase-measurement of a low level/low frequency signal superimposed on the upstream data. The ranging procedure is one of the challenging physical layer problems to be solved.
An other major aspect of the BAF network is the bursty nature of upstream traffic which requires a Burst Mode Receiver (BMR) in the LT. This receiver must be able to cope with large fluctuations in the data level, caused by variability in the network attenuation for different NT's. Currently AT&T is patenting this receiver.

3. Low level/low frequency ranging method principle

LT-NU distances can be 10 km maximum and 0 km minimum. Thus it is possible to have NU's at 0 km and NU's at 10 km from the LT within the same network. Because this possible difference in distance each NU has his own network attenuation and delay time. In the upstream direction this causes two problems. First we have the bursty character of the traffic due to the different attenuations and secondly we have collisions due to the different delay times.
The first problem is solved by developing a special Burst Mode Receiver, which is able to cope with the difference in received optical power.
A procedure is used to compensate for the different delay times, which is called ranging. The ranging procedure consists of three parts and the result of the ranging is that all NT's are on the same virtual distance, by installing an electronic delay-line at the NT.

The first part of the ranging procedure is the Static Coarse Ranging. The Static Coarse Ranging only takes place during installation of a NT and must determine the fibre delay with an inaccuracy of less than half a time slot. Hereafter we perform part two of the ranging procedure namely the Static Fine Ranging, which also only takes place during installation of a NT. If the inaccuracy of the static coarse ranging is more than a half time slot, then the static fine ranging will fail. This is allowed in 1% of the static coarse rangings. To start the static fine ranging the LT sends a commando to the NT under ranging, that the NT must transmit a Static Fine Ranging cell, consisting of a preamble in the middle of an idle time slot. The LT looks for this preamble and determines the delay with an inaccuracy of maximum 2 bits. Finally we have part three, the Dynamic Fine Ranging. Dynamic Fine Ranging is performed every time slot and is done by gap monitoring.
Looking at these three parts we see a clear difference in starting points of the delay between the first part and the last two parts. The last two parts, Static Fine Ranging and Dynamic Fine Ranging, know the delay with an accuracy enough to measure the delay via the data stream. If we want to perform the Static Coarse Ranging also via the datastream, then all the other NT's have to remain silent for a period of one round-trip time. The BAF-network has a maximum round-trip time of approximately 0.1 ms, so this would have some serious consequences for the network capacity and the data delay. That is why an "Out-of-band" method is preferred for the Static Coarse Ranging. "Out-of-Band" means that the ranging signals are outside the relevant frequency spectrum of the data, so the data traffic is able to continue during the Static Coarse Ranging.

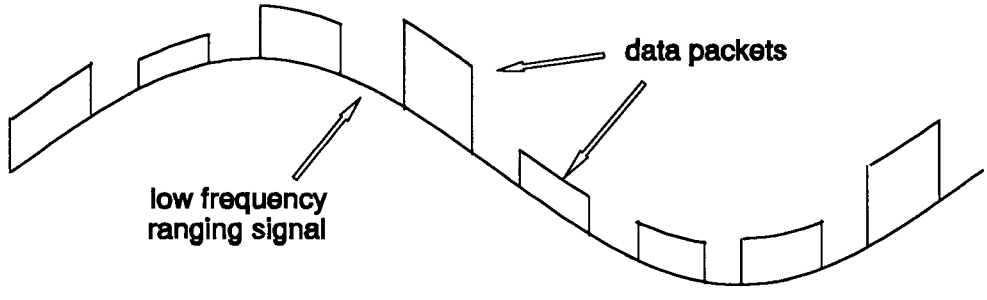

figure 3.1: upstream data and ranging signal

A new method for this Static Coarse Ranging which AT&T-NS-NL currently is patenting, has been proposed [1]. This method uses a low level, low frequency signal, which is superimposed on the upstream data traffic. An illustration of the upstream signal is shown in figure 3.1.
The received ranging signal at the LT is compared with a reference signal in the LT. The phase shift between these signals is a measure for the transmit delay. The principle of this low level/low frequency method is shown in figure 3.2.

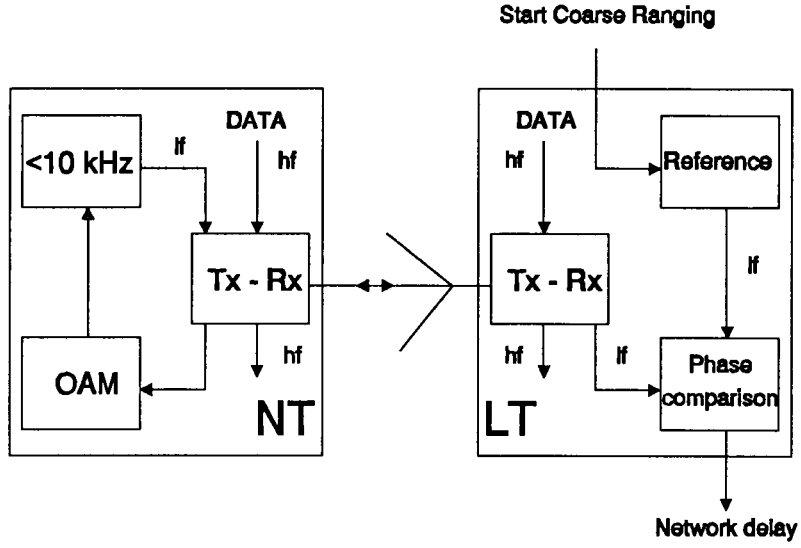

figure 3.2: low level/low frequency ranging method principle

The ranging signal is low level because we do not want it to interfere with the data signal (e.g. extra shot-noise in LT receiver). The mean power of the ranging signal at the transmitter is 10 dB (optical) down with respect to the mean power of the data at the transmitter. Next the ranging signal has a low frequency, first because we want it out of the data band and secondly we want an one to one relationship between phase and distance. This last requirement results in a ranging frequency less than 10 kHz (round-trip time is maximum 0.1 ms). There has been chosen for a sinusoidal signal, because a sinusoidal signal contains no higher frequency components. The higher frequencies can namely interfere with the data traffic and disturb the LT-receiver.
As shown in figure 3.2 the LT is sending downstream a command to the NT under ranging (via fast OAM-channel) with the message to start the ranging signal. This ranging signal starts with a pre-defined phase (e.g. 0). The LT knows when the command has been sent and starts the reference signal. After maximum one round-trip time (plus processing time in NT) the ranging signal has arrived at the LT and a phase comparison between ranging- and reference signal can be made. This phase shift is a measure for the network delay. After sending a delay adjust to the NT under ranging, the second step Static Fine Ranging is carried out. The Static Fine Ranging and Dynamic Fine Ranging are beyond the scope of this report. For information on Static and Dynamic Fine Ranging see [2].

4. Static Coarse Ranging Concept

Looking at figure 3.2 in chapter 3, we see two extra functions, which have to be implemented for static coarse ranging purposes. First at the NT-side a ranging signal generator has to be developed and secondly at the LT-side a reference signal and a phase comparison has to be designed.
In section 4.1 the principle of the ranging signal generator is described and in section 4.2 the extra functions at the LT-side are described.

4.1 Generation of the ranging signal in the NT

When a NT is being installed, but has not been ranged yet, the NT is already able to receive the downstream data. The static coarse ranging uses this possibility to give the NT the order to start the ranging signal. The LT sends to the NT under ranging via the fast OAM channel the command to start the generation of the ranging signal.
The ranging signal in the NT is derived from the data clock signal. If we derive the reference signal in the LT from the data clock signal also and we start the ranging signal in the NT with a pre-defined phase, then we are able to make a 'meaningful' phase comparison. The pre-defined phase has to be zero, because of the BMR structure.
When this ranging signal is generated digital, it is easy to start with a pre-defined phase. For this purpose a PROM and a Digital-to-Analog converter are used. The values of the ranging signal are stored in the PROM and this PROM is scanned with a clock signal derived from the data clock. Figure 4.1 shows the block diagram of this generation method.

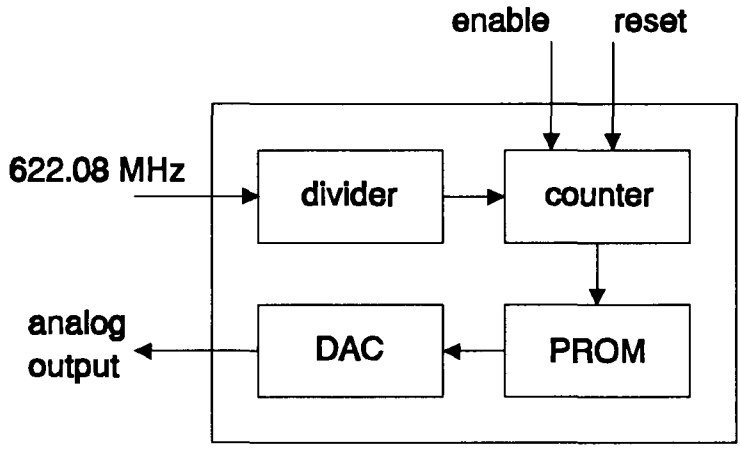

figure 4.1: block diagram of the ranging signal generation

The value for the divider is 64, so the scanning frequency is 7 times the slot clock, because one slot corresponds to 448 = 64·7 bits. The PROM-size is 1050 bytes and after scanning all these bytes one ranging signal period has passed, so the ranging frequency is 7/1050 times the slot clock, which is 9.257 kHz. This frequency is low enough to maintain the one to one relationship between phase and distance and creates a guard time of 8.0 µS (= $1/f_{ranging}$ - max. difference in delay = 108.0 - 100 µS) also.

4.2 Detection of the ranging signal in the LT

After the ranging signal has been generated in the NT and has been transported to the LT by the network, it is necessary to recover the ranging signal from the upstream traffic. Looking at figure 4.3 and keeping in mind that in reality the amplitude of the ranging signal is much smaller than the amplitude of the data packets and the variability of the amplitude of the data packets, then we understand that the data packets have an enormous influence on the ranging signal. An upstream BAF-cell consists of a 3 bytes preamble and an ATM cell of 53 bytes [2].

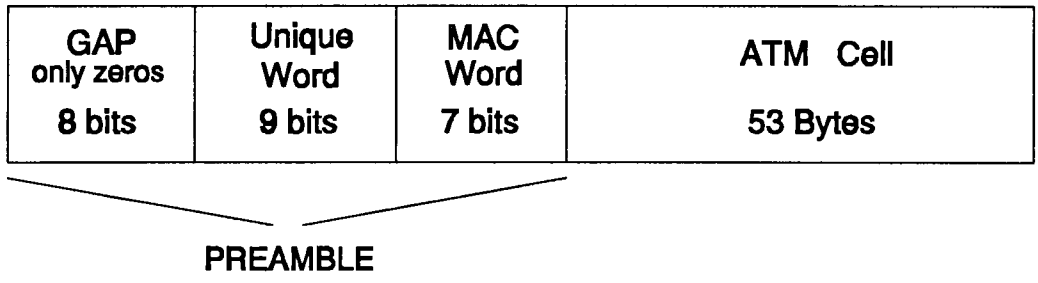

figure 4.2: Upstream BAF cell

As illustrated in figure 4.2 this preamble starts with 8 zeros followed by an Unique Word of 9 bits and a MAC word of 7 bits. The eight leading zeros are called the gap, because there is not really data present and necessary to reset the BMR. The Unique Word is used for bit/byte alignment and the MAC word contains information for the MAC protocol. So the only time in the upstream data, when there is not any data present, is during the gap. This gap is used gratefully to sample the ranging signal (figure 4.3).

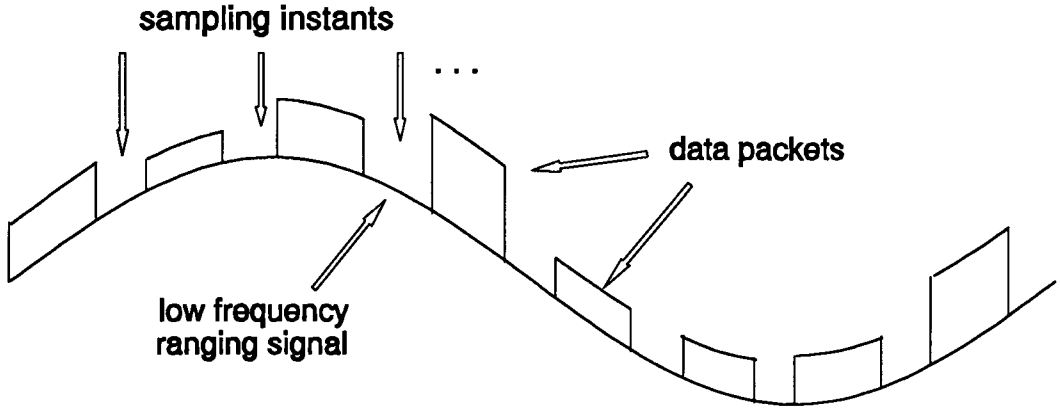

figure 4.3: sample instants at upstream data

The sample rate is equal to the slot rate, which is 1.39 MHz. This sample frequency is high enough to be able to reconstruct the ranging signal of 9.257 kHz, however the bandwidth of the noise, which is added to the signal, exceeds half the sample frequency. Normally this is not a problem, because you filter the input signal before sampling with a cut-off frequency of $\frac{1}{2}f_s$. But in our situation when you filter the upstream data with the ranging signal before sampling the power of the data packets will be spread out into the gap and the samples in the gap will also contain power of the data traffic.

Now a choice has to be made between aliasing of the noise and data interference. In section 5.1 the consequences of aliasing and data interference are described. The description of data interference in section 5.1 can be seen as a best case of data interference in case the upstream signal is filtered before sampling. If the aliasing and data interference figures are compared with each other, it is obvious that the data interference is much more serious. So, there has been decided to sample the signal without any form of filtering before sampling and take the aliasing for granted.

4.3 Phase comparison in the LT

After the sampling in the Burst Mode Receiver, the recovered ranging signal is fed to the static coarse ranging block. This block performs the phase comparison between the ranging signal and the reference signal. Three methods for phase comparison have been investigated and a short description of these methods, digital phase comparison with counter, digital phase comparison without counter and phase comparison with Discrete Fourier Transformation will be given in this section.

Digital phase comparison with counter
The block diagram of this method is shown in figure 4.4. The principle of operation is as follows: the zero-crossing of the reference signal is used to start the counter. The counter starts counting the system clock and it stops after the zero-crossing of the ranging signal. The value of the counter after the stop command represents the delay in number of data bits. This value is fed to a micro-processor (U-board controller) and this micro-processor calculates the average after several measurements.

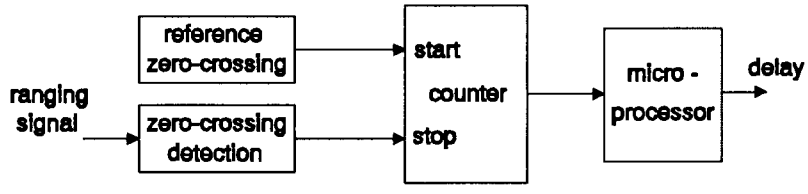

figure 4.4: block diagram of phase comparison with counter

The disadvantages of this method are that it is hard to measure the zero-crossing of a very noisy signal and only analog filtering can be adopted to improve the input signal. If we adopt analog filtering then we introduce an extra phase shift with an inaccuracy caused by a.o. temperature variation.

Digital phase comparison without counter
A block diagram of this method is given in figure 4.5.

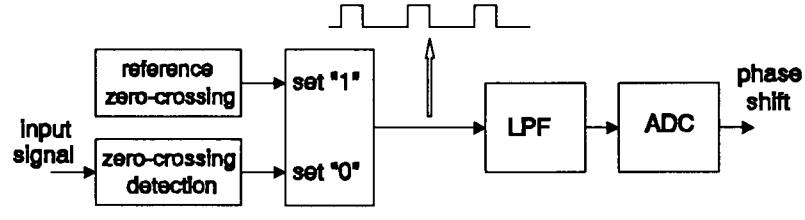

figure 4.5: block diagram phase comparison without counter

The operation of this method is as follows: the zero-crossing of the reference signal sets the output signal "high" (e.g. 5 V) and the zero-crossing of the ranging signal resets the output signal to "low" (e.g. 0 V). The duty cycle of this output signal is an indication of the phase shift. To determine the duty cycle of this signal we fed this output signal to a lowpass filter with a cut-off frequency of several Hertz and we measure the output voltage of this lowpass filter. This is done by an A/D converter. The output of the A/D converter represents the phase shift of the ranging signal.
This method has almost the same disadvantages as the previous method. First it is hard to measure the zero-crossing of a noisy signal and secondly the analog filter introduces an inaccurate extra phase shift.

Phase comparison with Discrete Fourier Transformation
Finally the third method which uses a discrete fourier transformation to determine the phase shift of the ranging signal. This discrete fourier transformation is performed by a micro-processor, so the analog ranging signal has to be converted to a set of digital values. The block diagram is shown in figure 4.6.

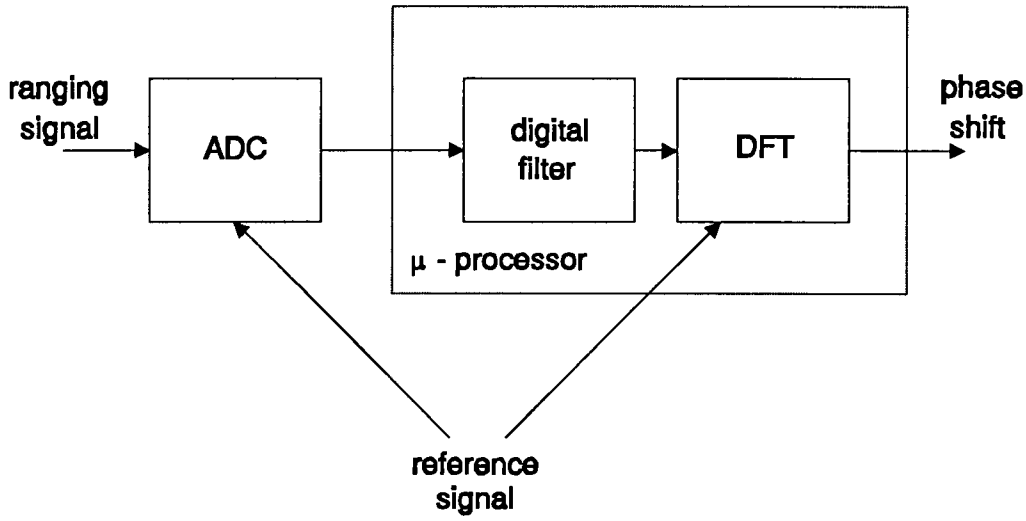

figure 4.6: block diagram phase comparison with DFT

The A/D converter samples the ranging signal and the samples are stored in a dedicated memory. After a number of samples the micro-processor performs some digital filtering and calculates the Fourier transformation coefficients of this signal for the ranging frequency. The argument of these coefficients is the phase shift of the ranging signal.
Because a digital filter is used instead of an analog filter, the phase shift caused by the filter is known exactly. This is one of the advantages of this method. A second advantage of this method is that it uses all the samples of the ranging signal and not only the zero-crossings. By this way more noise is filtered out. The larger amount of CPU-time, which is needed to perform the filtering and Fourier transformation, is a disadvantage of this method.
There are two options to implement this method of phase comparison. First the micro-processor which is already present on the board can be used and second specific hardware can be used to perform the filtering and Fourier transformation. The first option is chosen because software is much more flexible than hardware and second it requires less extra hardware. The extra amount of required CPU-time is not a real problem.

To prove that we can use discrete fourier transformation to determine the network delay, we look at the definition of the discrete fourier transformation:

$$X(n) = \sum_{k=0}^{N-1} x(k) \cdot e^{\frac{-j2\pi kn}{N}} \quad , \text{with } n=0,1,...,N-1 \tag{1}$$

Because we are only interested in the ranging frequency and a DFT window of one ranging period is taken and only the summation for n=1 has to be calculated. This yields:

$$\begin{aligned} X(1) &= \sum_{k=0}^{N-1} x(k) \cdot e^{\frac{-j2\pi k}{N}} \\ &= \sum_k x(k) \cdot \cos\left(\frac{2\pi \cdot k}{N}\right) - j \sum_k x(k) \cdot \sin\left(\frac{2\pi \cdot k}{N}\right) \end{aligned} \tag{2}$$

The received ranging signal x(k) can be described as:

$$x(k) = \sin\left(\frac{2\pi \cdot k}{N} + \Phi\right) \tag{3}$$

With Φ the phase delay caused by the network. Substituting eq. 3 in eq. 2 yields:

$$X(1) = \sum_{k=0}^{N-1} \frac{1}{2} \cdot \sin(\Phi) + \frac{1}{2} \cdot \sin\left(\frac{4\pi \cdot k}{N} + \Phi\right) - j \sum_k \frac{1}{2} \cdot \cos(\Phi) - \frac{1}{2} \cdot \cos\left(\frac{4\pi \cdot k}{N} + \Phi\right) \tag{4}$$

The summation of the terms with $4 \cdot \pi \cdot k/N + \Phi$ yields zero, so we find:

$$X(1) = \frac{N}{2} \cdot \sin(\Phi) - j \cdot \frac{N}{2} \cdot \cos(\Phi) \tag{5}$$

and the phase delay, Φ can be determined by the real and imaginair part of this Fourier transform.

Conclusion

The phase comparison method with the Discrete Fourier Transformation will be implemented, because it is very flexible, has few analog components and achieves a higher precision because it uses all the samples and not only the zero-crossings. It is flexible, because all the processing is done by software. The required CPU-time for this processing is not an essential problem. Because a digital filter is used instead of an analog filter, the phase shift caused by the filter is exactly known.

5. Inaccuracy of the DFT based method - Error sources

Unfortunately noise is added to the received ranging signal and the detection and comparison of the ranging signal are not ideal. But the static coarse ranging concept has been defined and so the error sources can be examined. In this chapter the error sources will be described and in the next chapter there influence on the phase measurement will be calculated.

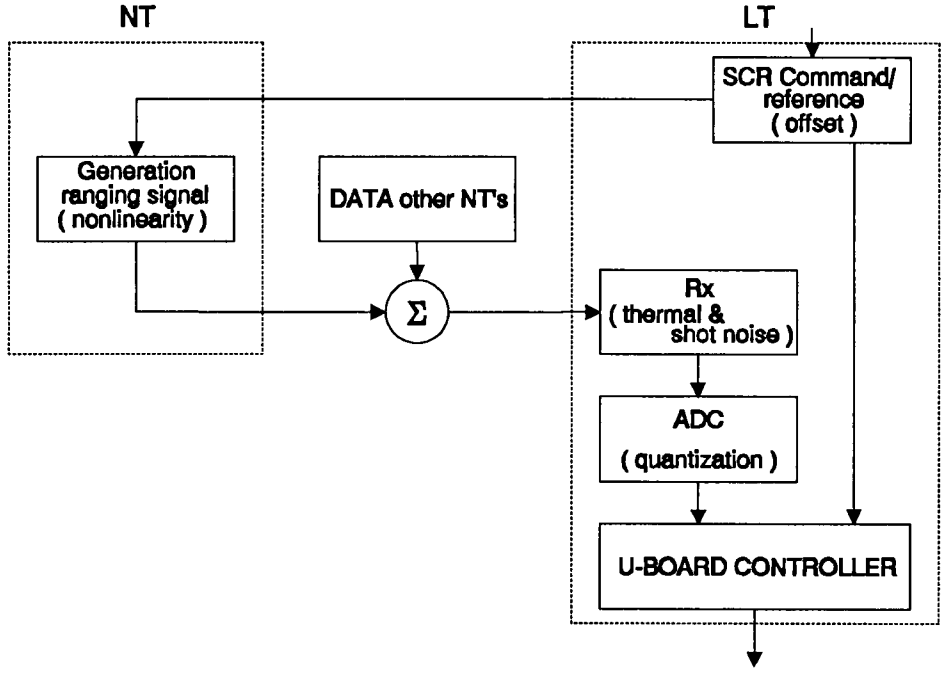

figure 5.1: Static Coarse Ranging route

In figure 5.1 the static coarse ranging route with the error sources is given. The error sources will be divided in two parts. The first part consists of the dynamic errors. With this are meant the disturbances that fluctuate during one coarse ranging process. If the coarse ranging process takes about 5 ms then this are the disturbances with a frequency of at least 200 Hz (e.g. thermal noise). These are described in section 5.1. The second group will be called the static errors. The static errors are disturbances that are almost constant during one coarse ranging process but can vary between different coarse ranging processes (e.g. phase shifts caused by temperature variation and variation in phase shift between different NT's caused by component tolerances) and these are described in section 5.2.

5.1 Dynamic error sources

Looking at figure 5.1 and keeping in mind the definition of dynamic errors, then we see four error sources, which belong to this category namely: thermal noise, shot noise, quantization noise and data interference.
Because we are interested in the Signal-to-Noise Ratio, first the minimum received ranging power is calculated.

Ranging signal

The transmitted ranging signal is 10 dB below the data level and the maximum network attenuation is 29.3 dB [2]. This results in a minimum received optical ranging power of -10 dBm - 29.3 dB = -39.3 dBm. For the electrical ranging signal power we find [3]:

$$S_{ranging} = (M \cdot R \cdot P_{mean})^2 \qquad (6)$$

With the multiplication factor of the APD, M is 10 and the responsivity of the APD in the 1300 nm window, R is 0.85 A/W. Substituting this values together with the ranging power (-39.3 dBm) in eq. 6 yields:

$$S_{ranging} = (10 \cdot 0.85 \cdot 10^{-6.93})^2 = -120.0\ dBA^2 \qquad (7)$$

Now the signal power can be compared with the different noise sources.

Thermal noise

First the thermal noise, this noise is caused by the LT receiver APD. The bandwidth of this thermal noise depends on the bandwidth of the receiver. In our situation the thermal noise has a bandwidth B of about 400 MHz and the density of this noise (i_{eq}) is about 15 pA/√Hz (= -216.5 dBA²/Hz). The total thermal noise becomes:

$$N_{thermal} = i_{eq} \cdot B = 9 \cdot 10^{-14}\ A^2 = -130.5\ dBA^2 \qquad (8)$$

But this is the thermal noise before sampling. As described in section 4.2 the ranging signal with noise is not filtered before sampling and because the bandwidth of the noise exceeds half the sample frequency, aliasing of the noise will occur. Because we are interested in the noise power after sampling, the influence of this aliasing has to be calculated. First we assume that $S_x(\omega)$ is the noise power spectrum of the input signal. In the Burst Mode Receiver (BMR) the signal is fed to a sample and hold circuit. For the noise power spectrum after sampling we find:

$$S_y(\omega) = \frac{1}{T}\sum_{k=-\infty}^{\infty} S_x\left(\omega - \frac{2\pi k}{T}\right) \qquad (9)$$

The sample frequency in the BMR is equal to the slot rate, which is 1.39 MHz. This yields T = 720.2 ns. For the thermal noise we assume a theoretical bandwidth of 800 MHz (-400 .. 400 MHz) and a power density η/2 (=η/4π per rad/s). Considering this the sum term in eq. 9 yields:

$$\sum_{k=-\infty}^{\infty} S_x\left(\omega - \frac{2\pi k}{T}\right) \approx \frac{800 \cdot 10^6}{1.39 \cdot 10^6} \cdot \frac{\eta}{4\pi} \quad ,\ for\ all\ \omega \qquad (10)$$

To calculate the average noise power of the output of the sample and hold circuit, first the mean square value of the samples is determined.

$$
\begin{aligned}
E\{|x[n]|^2\} &= \frac{1}{2\Omega}\int_{-\Omega}^{\Omega} S_y(\omega)d\omega \qquad , \Omega = \frac{\pi}{T} \\
&= \frac{T}{2\pi}\int_{-\pi/T}^{\pi/T} \frac{1}{T}\sum_k S_x\left(\omega - \frac{2\pi k}{T}\right)d\omega \\
&= \frac{T}{2\pi}\int_{-\pi/T}^{\pi/T} \frac{1}{T}\cdot\frac{800}{1.39}\cdot\frac{\eta}{4\pi}\,d\omega \\
&= 200\cdot 10^6\cdot\frac{\eta}{\pi}
\end{aligned}
\tag{11}
$$

The output signal is held at the sample value by the hold-circuit till the next sample, so the average energy of one sample is:

$$E\{|x[n]|^2\}\cdot T = 200\cdot 10^6\cdot\frac{\eta}{\pi}\cdot T = \frac{200}{1.39}\cdot\frac{\eta}{\pi}\ \ Ws \tag{12}$$

Because we want to know the average output noise power of the sample and hold circuit, the energy per sample is multiplied by the number of samples per second.
This yields for the average noise power:

$$N_{S/H} = energy/sample\cdot samples/\sec = \frac{200}{1.39}\cdot\frac{\eta}{\pi}\cdot f_s = 200\cdot 10^6\cdot\frac{\eta}{\pi}\ \ Watt \tag{13}$$

Comparing this with the average thermal noise power of the input signal:

$$N_{input} = \frac{1}{2\pi}\int_{-\infty}^{\infty} S_x(\omega)\,d\omega = \frac{1}{2\pi}\int_{-2\pi\cdot 4\cdot 10^8}^{2\pi\cdot 4\cdot 10^8}\frac{\eta}{4\pi}\,d\omega = 200\cdot 10^6\cdot\frac{\eta}{\pi}\ \ W \tag{14}$$

We see that the thermal noise power in the sampled signal (eq. 13) and in the input signal (eq. 14) are equal and thus in our situation after sampling we have:

$$N_{thermal,\ afterS/H} = -130.5\ dbA^2 \tag{15}$$

The noise output signal of the sample and hold circuit is shown in figure 5.2 and is a random digital wave with zero-mean and $\sigma = \sqrt{N}$. The spectral density of the noise is given by [4]:

$$
\begin{aligned}
S(f) &= \sigma^2\cdot T_s\cdot sinc^2(f\cdot T_s) \\
&= 6.4\cdot 10^{-20}\cdot sinc^2(7.2\cdot 10^{-7}\cdot f)
\end{aligned}
\tag{16}
$$

and is shown in figure 5.3. The noise density for the lower frequencies increases and becomes -191.9 dBA^2/Hz.

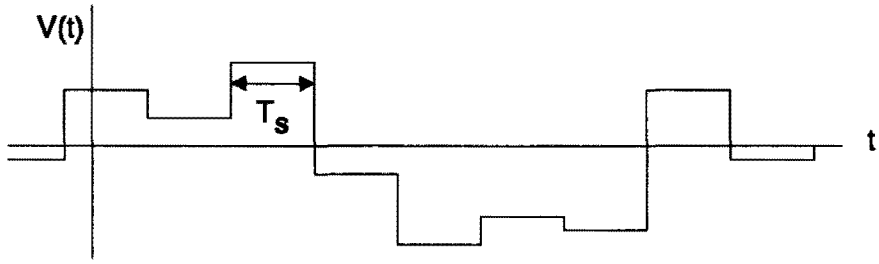

figure 5.2: Example of noise signal after sample and hold circuit

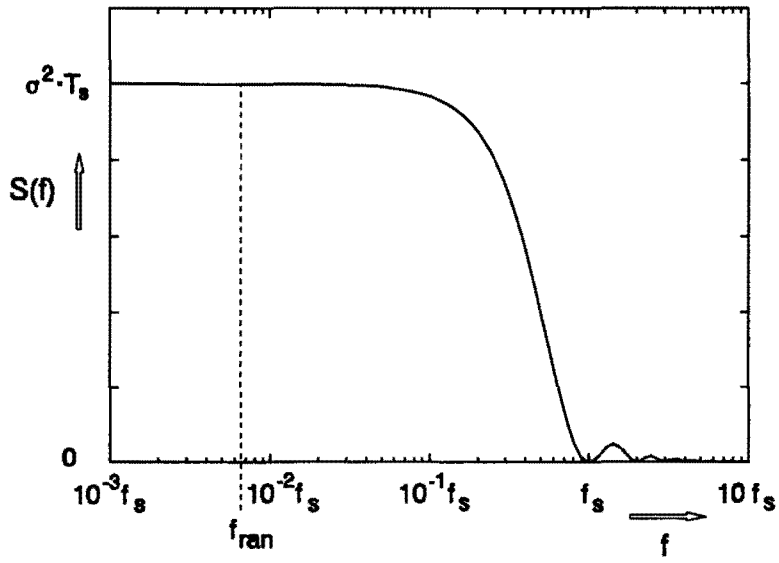

figure 5.3: Noise density after sample and hold circuit

Shot noise
Secondly the shot noise, for this noise we find [3]:

$$N_{shot} = 2 \cdot q \cdot R \cdot P_{mean} \cdot M^2 \cdot F \cdot B \quad [A^2] \tag{17}$$

Where q is $1.6 \cdot 10^{-19}$, R the responsivity of the APD in the 1300 nm window is 0.85 A/W, P_{mean} the mean received power, M the multiplication factor of the APD is 10, F the excess noise factor is $M^{0.7}$ and B the bandwidth is 400 MHz. If we assume that during the gap only the NT under ranging is transmitting, then P_{mean} is:

$$P_{mean} = \frac{P_{transmitted}}{Network\ attenuation} = -10dBm - 29.3dB = -39.3dBm \tag{18}$$

Substitution of eq. 18 in eq. 17 yields:

$$N_{shot} = 6.41 \cdot 10^{-15}\ A^2 = -141.9\ dBA^2 \tag{19}$$

If the network attenuation is less than 29.3 dB then P_{mean} will increase and the shot noise will increase. However the electrical ranging signal power increases with P_{mean}^2 and the shot noise only with P_{mean}, so the Signal-to-Noise ratio improves when the network attenuation decreases.
Comparing the shot noise (eq. 17) with the thermal noise (eq. 15), we find that the shot noise is small with respect to the thermal noise if the network attenuation is more than 18 dB and of the same kind of magnitude if the network attenuation is less than 18 dB.
The influence of the sample and hold circuit on the shot-noise is analog to the influence on the thermal noise. Thus the shot-noise power after the sample and hold is equal to the input shot-noise power and the shot-noise density for the lower frequencies increases.

Quantization noise
In the third place the quantization noise, after sampling in the burst mode receiver the sample is converted from analog to digital. This conversion adds quantization noise and this noise depends on the resolution of the A/D convertor. The quantization error is uniform distributed over the interval [-½LSB, +½LSB] with the variance:

$$\sigma^2 = \frac{1}{12}\cdot(½-(-½))^2 = \frac{1}{12} \qquad (20)$$

If the A/D converter uses n LSB's for the ranging signal, then the ranging signal power is:

$$P_{ranging} = \frac{(Amplitude)^2}{2} = \frac{1}{2}\cdot\left(\frac{n}{2}\right)^2 = \frac{n^2}{8} \qquad (21)$$

This yields a Signal-to-Noise Ratio (SNR) of:

$$SNR_{ADC} = \frac{P_{ranging}}{\sigma^2} = \frac{3}{2}\cdot n^2 \text{ , } n \text{ is the total number of used LSB's} \qquad (22)$$

The maximum difference in network attenuation and thus the maximum difference in $V_{t\text{-}t}$ of the ranging signal is 15 dB (factor 32). If we take a 12 bits A/D convertor and match the input range of the A/D converter with the maximum ranging $V_{t\text{-}t}$ (for min. network attenuation), then there are 7 bits left for the minimal $V_{t\text{-}t}$. Seven bits correspond to $n = 2^7 = 128$ steps. Substituting this value in eq. 20 yields:

$$SNR_{ADC} = \frac{3}{2}\cdot 128^2 = 43.9\ dB \qquad (23)$$

This means that the power of the quantization noise which is added, is more than 43.9 dB below the smallest ranging signal power. The ranging signal power for the minimal $V_{t\text{-}t}$ is -120 dBA^2 (eq. 7), so the quantization noise is maximum -163.9 dBA^2. If we use sufficient bits (e.g. 12) the quantization noise is negligible with respect to the thermal noise.
An other similar noise source is the restricted wordlength in the U-board controller. However the U-board controller uses 32 bits internally, so this noise is negligible with respect to the other noise sources.

Data interference

Finally we describe the data interference. In section 4.2 we said that the samples are taken during the gap, so there should not be any data interference. But there was a possibility that the laser of the next NT to transmit already is in a prebias-state during the gap. This prebias-state is perhaps necessary to warm-up the laser. The power sent by a laser in the prebias-state is equal to the 'zero' level of his data. The main problem with the prebias-state is caused by the difference in received 'prebias-state' power. The network attenuation for the different NT's can namely vary about 15 dB.

We assume the NT's to transmit in random order, so in worst case we have a NT at 0 km and a NT at 10 km transmitting by turn. If we assume the received prebias-state power of the NT at 10 km is zero and of the NT at 0 km is A then the received interference signal looks like figure 5.4.

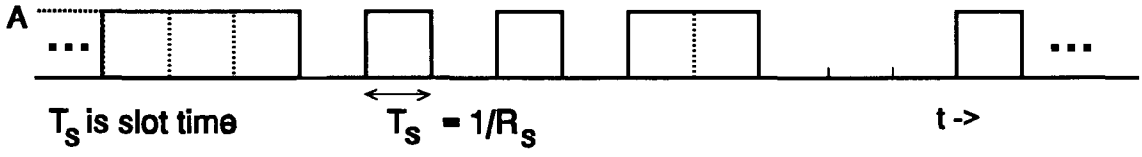

figure 5.4: Example of interference signal

The spectral density of a random binary digital wave with peak-peak amplitude A is:

$$S(f) = \frac{A^2}{2 \cdot R_s} \cdot sinc^2\left(\frac{f}{R_s}\right) + \frac{A^2}{4}\delta(f) \qquad , f \geq 0 \text{ and } R_s \text{ is the slot rate} \tag{24}$$

and the noise power of the interference signal is:

$$N_{interference} = \int_{f^-}^{f^+} \frac{A^2}{2 \cdot R_s} \cdot sinc^2\left(\frac{f}{R_s}\right) + \frac{A^2}{4}\delta(f)\, df \tag{25}$$

with $A = M \cdot R \cdot P_{prebias\ NT\ at\ 0\ km}$, where M = 10 the multiplication factor of the APD and R the responsivity of the APD, which is 0.85 A/W and with f^+ and f^- the upper and lower end of the noise bandwidth. The slot rate is $622.08 \cdot 10^6/448 = 1.39 \cdot 10^6$ slots/s.

If we know $P_{prebias}$ of the NT at 0 km then we know A and we are able to calculate the noise density. For the NT at 0 km we have a minimum network attenuation of 14.5 dB and the prebias level is equal to the 'zero' data level, which is -9.5 dBm [2]. This yields a received prebias power of -24.0 dBm. Substitution of this value in eq. 24 yields a noise power density of η = -154.5 dbA^2/Hz for frequencies smaller than 100 kHz and for the total ac-power of the interference signal (eq. 25) we find:

$$N_{interference} = \frac{A^2}{4} = -95.4\ dBA^2 \tag{26}$$

Comparing this with the other noise and the ranging signal, we see that the influence of the interference signal is enormous (SNR = -24.6 dB). That is why is decided to turn the lasers off during the gap.

5.2 Static error sources

Because of the fact that the static errors have not almost zero mean during one coarse ranging process, these category of errors is worse than the dynamic errors. Three error sources belong to this category: a phase shift between the LT transmitter and LT receiver slot clock (offset), variation of components due to temperature variation or component tolerances and the non-linearity of the NT laser.

Offset
In [5] the timing of the U-interface board is described and there is depicted that the transmitter slot-clock in the LT and the receiver slot-clock in the LT need not to be phase synchronized. The receiver slot-clock, used for the BMR and the ranging block, is initialized by the transmitter slot-clock which is used for the outgoing data stream, but is clocked by a 80 MHz clock. Because of this a phase shift between transmitter and receiver slot-clock of 1 byte might occur and this phase shift is not measured.
The sampling of the ranging signal is clocked by the receiver slot-clock, however the start pulse of the Static Coarse Ranging is triggered by the transmitter slot-clock, so we have an inaccuracy in the absolute phase delay measurement of 1 byte, caused by this unknown phase difference. However the entire ranging procedure for all the NT's is related to the receiver slot-clock, thus all NT's have the same offset and this absolute inaccuracy gives no trouble for the ranging. The devices on the U-board which have to know the absolute delay only require an accuracy of half a timeslot (28 bytes) and also do not suffer from this phase offset.

Component variations
In the BAF-network we have maximum 32 NU's, that have to be ranged by one LT. The start coarse ranging command is sent to the NU by the LT via the Fast OAM channel and the NU has to recognize this command. After receiving this command the NU starts the ranging signal generation. The NU needs a certain time to process the static coarse ranging start command. Because the coarse ranging is used to determine the fibre delay, we have to correct the ranging result for this processing time, which is part of the ranging loop. If this time is constant then the problem is similar to the slot-clock offset and only causes an error in the measured absolute delay. However the processing time is not constant because of temperature variation and tolerances of components used for the different NU's.
This processing time has been specified at 120 ± 6 ns. This maximum variation of 12 ns corresponds to 7.5 bits and the coarse ranging result will always be affected by this inaccuracy.
At the NU we saw that the variations were caused by temperature variation and component variation. Because the system only has one LT there are no problems with component tolerances at the LT-side. The problem caused by temperature variation lies in the sample-and-hold circuit of the Burst Mode Receiver and has been specified at 6 ns. This variation corresponds to 3.7 bits.

Laser non-linearity

Finally the non-linearity of the NU-laser which results in the presence of higher harmonics. When the ranging signal in the BMR is sampled, aliasing of the input signal occurs and the higher harmonics can interfere with the ranging signal. These higher harmonics are mainly caused by the transition from led to laser operation of the laser. In figure 5.5 an ideal laser characteristic is depicted.

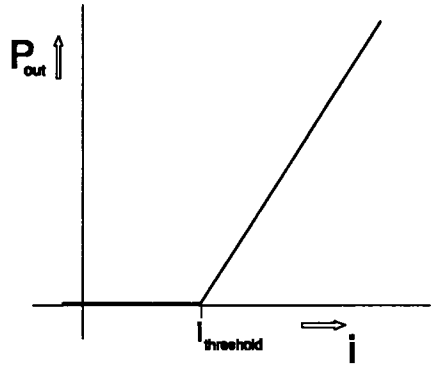

figure 5.5: Ideal laser characteristic

If we modulate this ideal laser with a sinusoidal signal and a part of this signal drives the input current below the thresholdpoint, then the output signal looks like figure 5.6. This effect is called bottoming of the output signal.

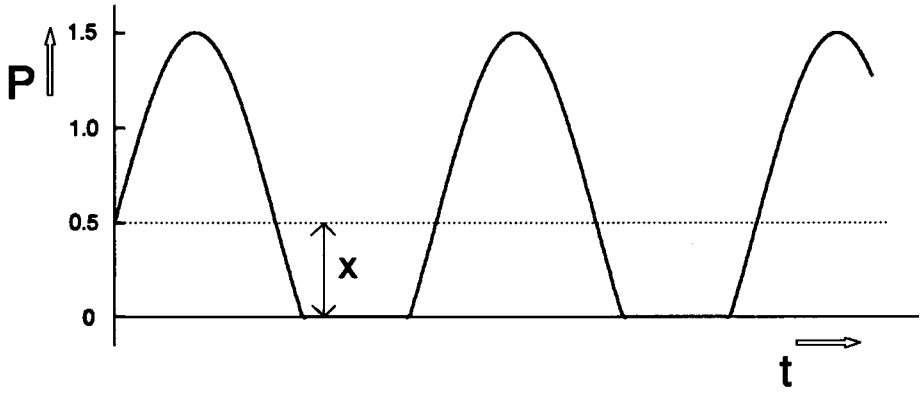

figure 5.6: Output signal, laser operating near the threshold point

We assume the amplitude to be unity and that the signal at the bottom is limited at x down the mean value of the sinusoidal signal (-1<x<1). This signal can be described by:

$$f(t) = \begin{cases} 0, & \frac{T}{2\pi}(\pi - a\sin(-x)) < t < \frac{T}{2\pi}(a\sin(-x) + 2\pi) \\ \sin(\omega_0 t) + x, & \frac{T}{2\pi}a\sin(-x) < t < \frac{T}{2\pi}(\pi - a\sin(-x)) \end{cases} \qquad (27)$$

and $f(t+T) = f(t)$, $\omega_0 = \frac{2\pi}{T}$.

This signal f(t) can also be described by the Fourier Series:

$$f(t) = \frac{1}{2}a_0 + \sum_{n=1}^{\infty}(a_n\cos(n\omega_0 t) + b_n\sin(n\omega_0 t)) \tag{28}$$

If we calculate the coefficients a_0, a_n and b_n then we can evaluate the harmonic distortion caused by an ideal laser.
First let us consider a_0:

$$a_0 = \frac{2}{T}\int_{-T/2}^{T/2} f(t)\,dt \tag{29}$$

Looking at eq. 27 we define:

$$t_1 = \frac{T}{2\pi}asin(-x) \tag{30}$$

and

$$t_2 = \frac{T}{2\pi}(\pi - asin(-x)) \tag{31}$$

If we substitute eq. 27, eq. 30 and eq. 31 in eq. 29 then we find for a_0:

$$\begin{aligned} a_0 &= \frac{2}{T}\int_{t_1}^{t_2}\left(\sin(\omega_0 t) + x\right)dt \\ &= \left(-\frac{2}{T}\cdot\frac{1}{\omega_0}\cos(\omega_0 t) + \frac{2}{T}\cdot x\cdot t\right)\Big|_{t_1}^{t_2} \\ &= \frac{2}{\pi}\sqrt{1-x^2} + \frac{x}{\pi}(\pi - 2asin(-x)) \end{aligned} \tag{32}$$

After calculating the 'dc'-component of the laser output signal, the fourier coefficients a_n with n=1,2,3,.. are calculated:

$$\begin{aligned} a_n &= \frac{2}{T}\int_{-T/2}^{T/2} f(t)\cdot\cos(n\omega_0 t)\,dt \\ &= \frac{2}{T}\int_{t_1}^{t_2}\sin(\omega_0 t)\cdot\cos(n\omega_0 t)\,dt + \frac{2}{T}\int_{t_1}^{t_2} x\cdot\cos(n\omega_0 t)\,dt \end{aligned} \tag{33}$$

This is split into two integrals and first the left integral is calculated:

$$\frac{T}{2}\int_{t_1}^{t_2}\sin(\omega_0 t)\cdot\cos(n\omega_0 t)\,dt = \frac{1}{T}\int_{t_1}^{t_2}\sin[(1+n)\omega_0 t]+\sin[(1-n)\omega_0 t]\,dt$$

$$= -\frac{1}{T}\cdot\left\{\frac{\cos[(1+n)\omega_0 t]}{(1+n)\omega_0}+\frac{\cos[(1-n)\omega_0 t]}{(1-n)\omega_0}\right\}\Bigg|_{t_1}^{t_2}$$

$$= \frac{1}{2\pi}\cdot\left\{\frac{(-1)^n\cos[(1+n)asin(-x)]+\cos[(1+n)asin(-x)]}{(1+n)}+\right. \tag{34}$$

$$\left.\frac{(-1)^n\cos[(1-n)asin(-x)]+\cos[(1-n)asin(-x)]}{(1-n)}\right\}$$

$$= \begin{cases} 0, & n \text{ is odd} \\ \frac{1}{\pi}\cdot\left(\frac{\cos[(1+n)asin(-x)]}{(1+n)}+\frac{\cos[(1-n)asin(-x)]}{(1-n)}\right), & n \text{ is even} \end{cases}$$

For the right integral is found:

$$\frac{2}{T}\int_{t_1}^{t_2}x\cdot\cos(n\omega_0 t)\,dt = \frac{2x}{Tn\omega_0}\sin(n\omega_0 t)\Big|_{t_1}^{t_2}$$

$$= \frac{x}{\pi n}\cdot[\sin(n\pi - n\cdot asin(-x)) - \sin(n\cdot asin(-x))]$$

$$= \frac{x}{\pi n}\cdot[(-1)^{n+1}\sin(n\cdot asin(-x)) - \sin(n\cdot asin(-x))] \tag{35}$$

$$= \begin{cases} 0, & n \text{ is odd} \\ \frac{-2x}{\pi n}\cdot\sin(n\cdot asin(-x)), & n \text{ is even} \end{cases}$$

Substituting eq. 34 and eq. 35 in eq. 33 yields for a_n:

$$a_n = \begin{cases} 0, & n \text{ is odd} \\ \dfrac{-2x\sin[n\,asin(-x)]}{\pi n} + \dfrac{\cos[(1+n)asin(-x)]}{(1+n)\pi} + \dfrac{\cos[(1-n)asin(-x)]}{(1-n)\pi}, & n \text{ is even} \end{cases} \tag{36}$$

Similarly for the coefficients b_n,

$$\begin{aligned} b_n &= \frac{2}{T}\int_{-T/2}^{T/2} f(t)\cdot\sin(n\omega_0 t)\,dt \\ &= \frac{2}{T}\int_{t_1}^{t_2} \left(\sin(\omega_0 t)+x\right)\cdot\sin(n\omega_0 t)\,dt \end{aligned} \tag{37}$$

When n = 1,

$$b_1 = \frac{1}{2} - \frac{asin(-x)}{\pi} + \frac{\sin[2\,asin(-x)]}{2\pi} + \frac{2x\cos[asin(-x)]}{\pi} \tag{38}$$

When n = 2, 3, ... ,

$$b_n = \begin{cases} 0, & n \text{ is even} \\ \dfrac{2x\cos[n\,asin(-x)]}{\pi n} + \dfrac{\sin[(1+n)asin(-x)]}{(1+n)\pi} - \dfrac{\sin[(1-n)asin(-x)]}{(1-n)\pi}, & n \text{ is odd} \end{cases} \tag{39}$$

Now, we have a definition for all fourier coefficients and we are able to calculate the harmonic distortion caused by the threshold of an ideal laser. In figure 5.8 the higher harmonics with respect to the ranging signal for different values of x are shown.
This is the harmonic distortion for an ideal laser. But what will be the changes when we take a more realistic laser characteristic?

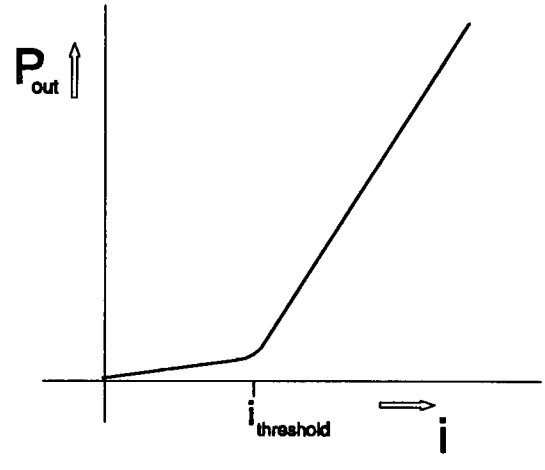

figure 5.7: more practical laser characteristic

Looking at figure 5.7 we see a more practical laser characteristic and this shows us two differences. First, the part below the threshold is not zero, but has a small slope and second, the transition from led to laser operation is not that sharp. These differences provide a smaller harmonic distortion, because the sinusoidal signal is not cut sharp but the lowest part of the signal is attenuated. So the figures for harmonic distortion of an ideal laser can be treated as a worst case for a more practical laser.

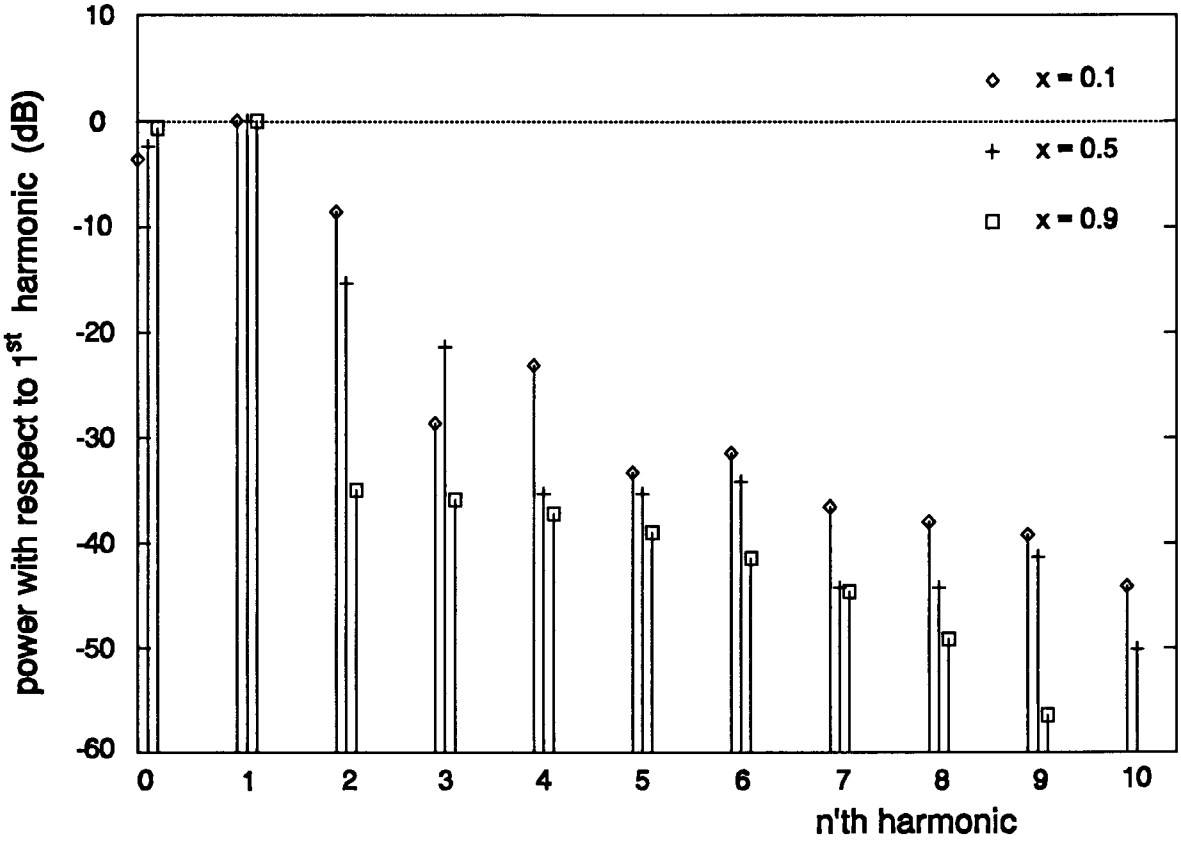

figure 5.8: Harmonic distortion of an ideal laser

Harmonic distortion measurement

To verify the estimation of the harmonic distortion caused by the transmitter laser a measurement has been performed. The measurement set-up is shown in figure 5.9.

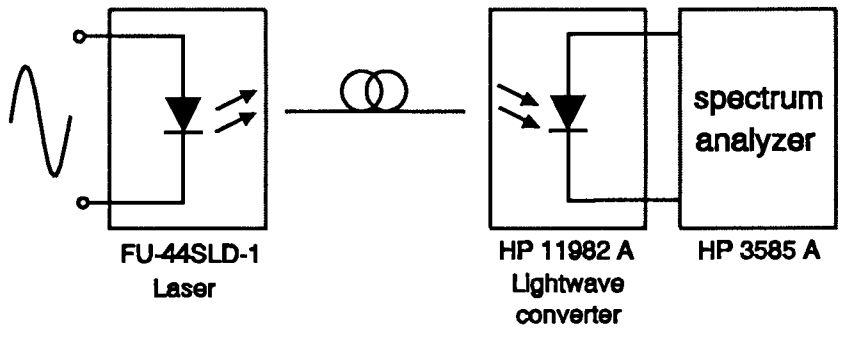

figure 5.9: Measurement set-up for harmonic distortion

The laser module (mitsubishi FU-44SLD-1, appendix 5) is also used in the NU. The measurement has been performed for several values of x which is the ratio between threshold-offset and the amplitude of the input signal (see fig. 5.10 and fig. 5.6).

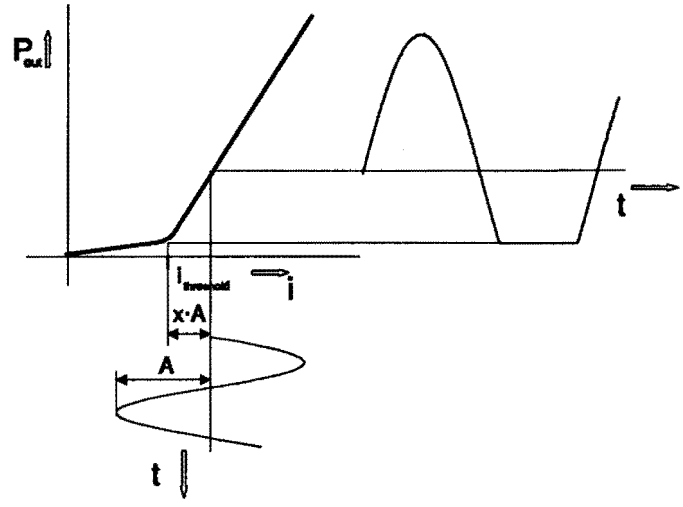

figure 5.10: Input and output signal of the laser module

The results for the measurements with x=0.9, 0.5 and 0.1 are depicted in fig. 5.11, 5.12 and 5.13 together with the theoretical values for an ideal laser.

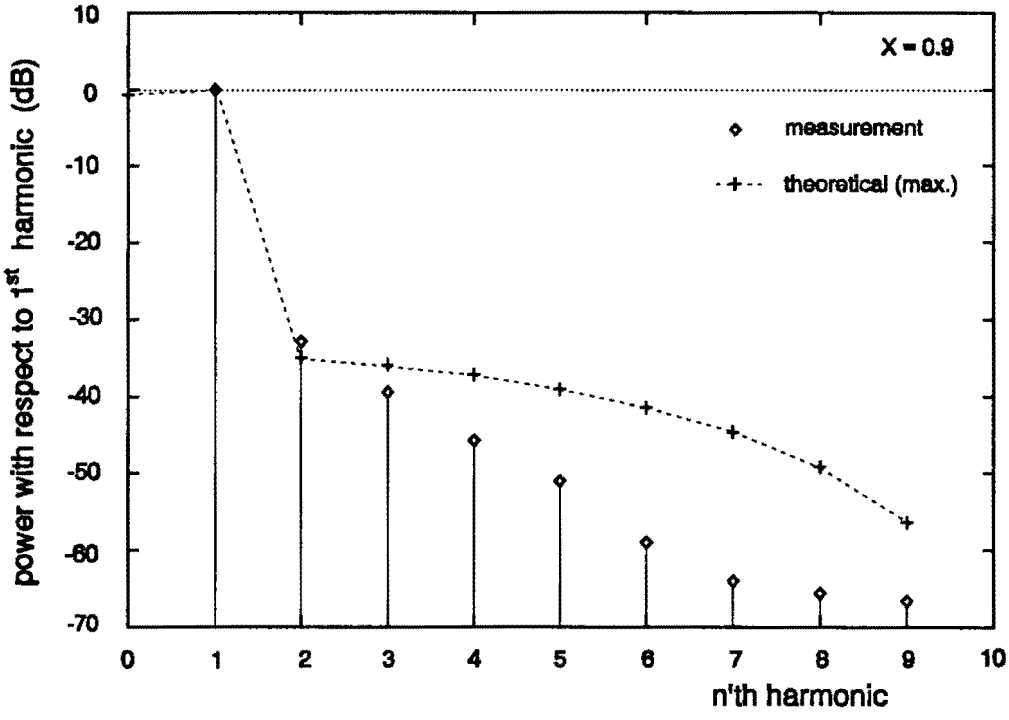

figure 5.11: Measurement results of higher harmonics for x = 0.9

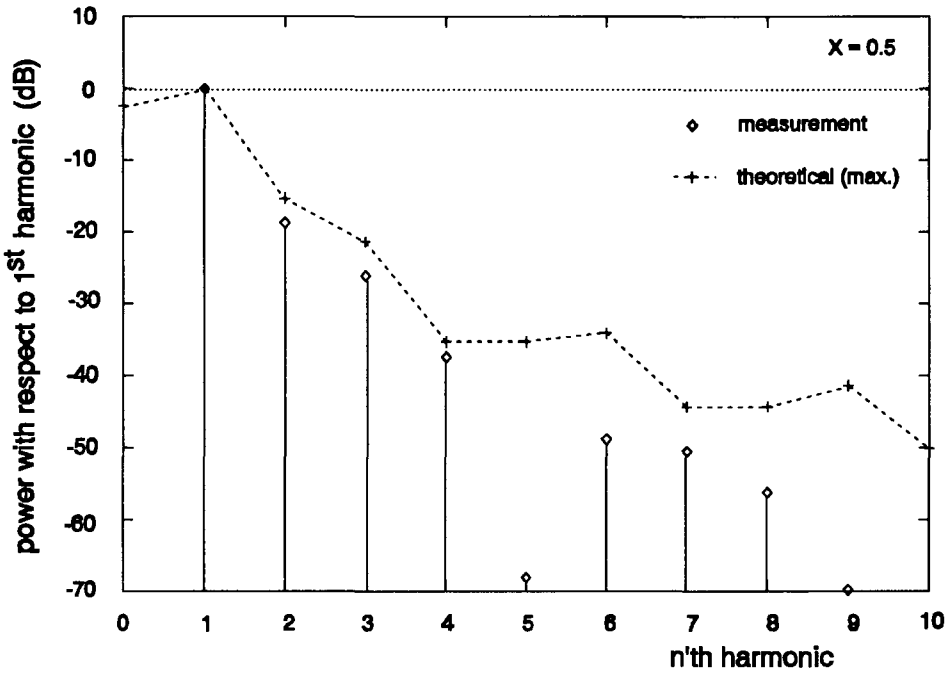

figure 5.12: Measurement results of higher harmonics for x = 0.5

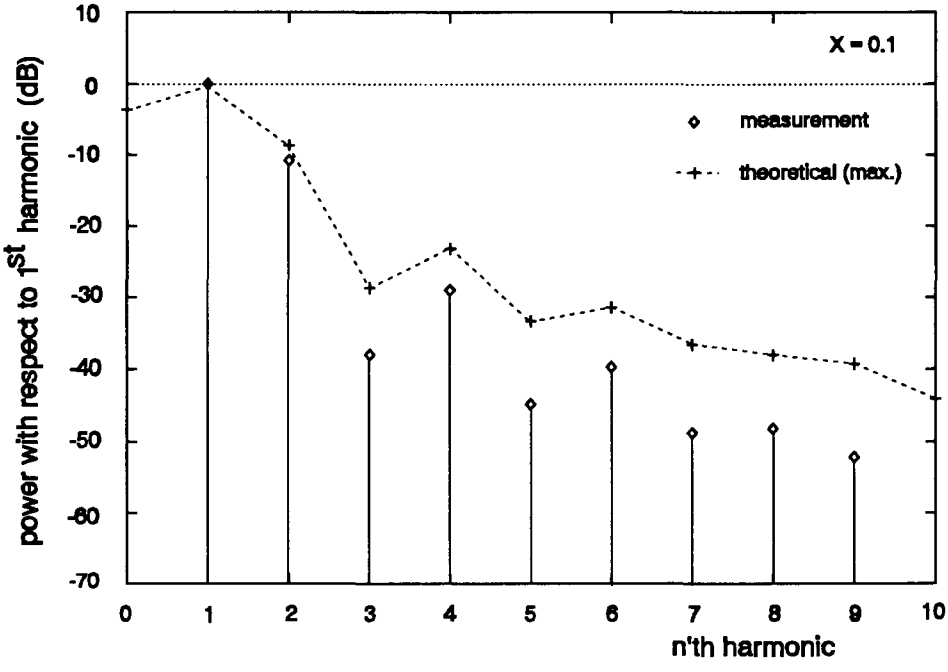

figure 5.13: Measurement results of higher harmonics for x = 0.1

There has been described that for a practical laser the calculated figures can be treated as worst case. Looking at the figures 5.11, 5.12 and 5.13 a close agreement between the measurement results and the theoretical maximum is found. The assumption that the calculated figures for an ideal laser are a worst case for a practical laser are justified.

6. Inaccuracy of the DFT based method - Estimation

In this section the attainable accuracy of the chosen system is discussed. The digital signal processing algorithm implementation plays a major roll in this. With help of the error source descriptions in the previous section and selection criteria, like required CPU-time and performance, a choice is made for the digital signal processing software implementation. Finally the accuracy of the chosen method will be calculated.
Before looking at several algorithms, the aliasing effect of the higher harmonics and the filtering effect of the DFT part are considered.

6.1 Aliasing of the higher harmonics

The static coarse ranging circuit samples the ranging signal 150 times each ranging period and stores the values in a dedicated memory. Next the samples are being used to compute the phase of the received ranging signal and as described in section 4.3 Discrete Fourier transformation techniques will be used for this purpose.
When the ranging signal is converted from a continuous signal to a discrete signal aliasing of the noise will occur. The consequences of this aliasing are described in section 5.1. Besides the aliasing of noise also aliasing of the higher harmonics may occur. We will derive a relation between the number of samples per ranging period and the higher harmonics which can influence the phase measurement.
Assume a periodic signal x(t), which can be expressed by a fourier series representation. In the time continuous situation the Fourier coefficients a_n and b_n can be computed as:

$$a_n = \frac{2}{T}\int_0^T x(t)\cdot\cos(2\pi nft)\,dt$$
$$b_n = \frac{2}{T}\int_0^T x(t)\cdot\sin(2\pi nft)\,dt \qquad (40)$$

where T = 1/f is the period of signal x(t). For a discrete system eq. 40 can be expressed as:

$$a_n^d = K\sum_{i=0}^{N-1} x(i\Delta T)\cdot\cos(2\pi nfi\Delta T)$$
$$b_n^d = K\sum_{i=0}^{N-1} x(i\Delta T)\cdot\sin(2\pi nfi\Delta T) \qquad (41)$$

Where K is the proportionality constant, ΔT is the sampling interval and $N = T/\Delta T$ is the number of samples taken every cycle of signal x(t).

Applying the theory of signal processing [6] it could be easily proved that the relationship between the coefficients of the analog and discrete systems is:

$$a_n^d = \frac{1}{\Delta T} \sum_{m=-\infty}^{\infty} a_{n+mN}$$
$$b_n^d = \frac{1}{\Delta T} \sum_{m=-\infty}^{\infty} b_{n+mN} \qquad (42)$$

Figure 6.1(a) shows the frequency response of the periodic signal x(t). Figure 6.1(b) and 6.1(c) show the frequency responses of the discrete signal x(iΔT), $0 \le i \le N-1$. In figure 6.1(b), N>2h (h is highest harmonic of signal x(t)) but in figure 6.1(c), N<2h. The sampling rate in figure 6.1(c) is less than the Nyquist sampling rate. Thus aliasing effect is seen on the frequency response shown in figure 6.1(c).

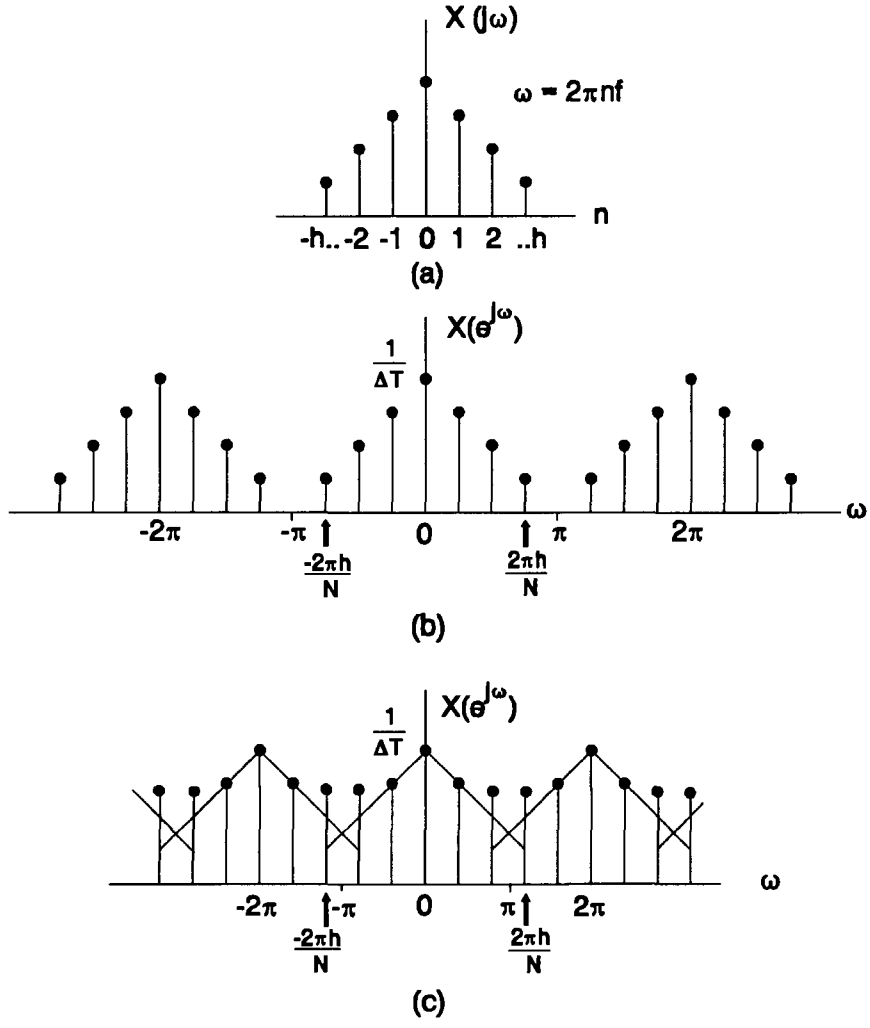

figure 6.1: (a) Frequency response of the analog signal x(t). (b) Frequency response of the discrete signal x(iΔT), $0 \le i \le N-1$, with $N > 2h$. (c) Frequency response of the discrete signal x(iΔT), $0 \le i \le N-1$, with $N < 2h$.

The phase associated with the 1st harmonic (fundamental phase) of x(t) can be accurately measured from the samples x(iΔT), $0 \leq i \leq N-1$, if the ratios b_1^d/a_1^d, and b_1/a_1 are identical. These ratios will be the same if there is no aliasing effect on the 1st harmonic response. If all the harmonics i, $2 \leq i \leq h$, are present in signal x(t), then from figure 6.1(c) it is clear that the 1st harmonic will not be affected by the aliasing effect if $(2\pi - 2\pi h/N) > 2\pi/N$, i.e., if $N > h+1$. In other words the 1st harmonic can be affected by the n^{th} harmonics for $n > N-1$. Looking at eq. 42 we find that the 1st harmonic will be affected by the n^{th} harmonics with $n = 1 + iN$ and i is an integer.

6.2 Filtering by the Discrete Fourier Transformation

The Discrete Fourier Transformation is used to determine the phase of the ranging signal. This method results in a higher precision with respect to other methods, which only use the zero-crossings of a signal, because the DFT also filters the signal. In this section the transfer function of the DFT will be derived. This transfer function can be used to calculate the improvement on the Signal-to-Noise Ratio.
When the Fourier transformation is considered with a DFT-window of m ranging periods and the output is called y, then the discrete output signal can be expressed as:

$$y(kT) = \sum_{l=-\infty}^{\infty} x[l\tau] \cdot h[kT - l\tau] \tag{43}$$

where $T = m \cdot T_{ranging}$ is the DFT window size and $\tau = T_s$ is the interval time between two samples. This equation is the convolution of x[n] and h[n], thus the Fourier transform of h[n], H(ω), is the transfer function of the DFT. For h[n] we find:

$$h[n] = \left(u[n+\frac{T}{2\tau}] - u[n-\frac{T}{2\tau}]\right) \cdot e^{\frac{j2\pi n\tau}{T_{ranging}}} \tag{44}$$

The Fourier transform of the part between brackets is given by [7]:

$$H(e^{j\theta}) = \frac{\sin(\frac{T}{\tau} \cdot \frac{\theta}{2})}{\sin(\frac{\theta}{2})} \tag{45}$$

where $\theta = \omega \cdot \tau$ is the normalized frequency and $T/\tau = N \cdot m$ is the total number of used samples. The second part of eq. 44 is a multiplication by $e^{jn\nu}$ and in the frequency domain this yields a phase shift of ν. The Fourier transform of h[n] becomes:

$$H(e^{j\theta}) = \frac{\sin(\frac{T}{\tau} \cdot \frac{\theta - \nu}{2})}{\sin(\frac{\theta - \nu}{2})} \tag{46}$$

where $\nu = \omega_{ranging} \cdot \tau$ is the frequency shift. In figure 6.2 the transfer function of the DFT is shown.

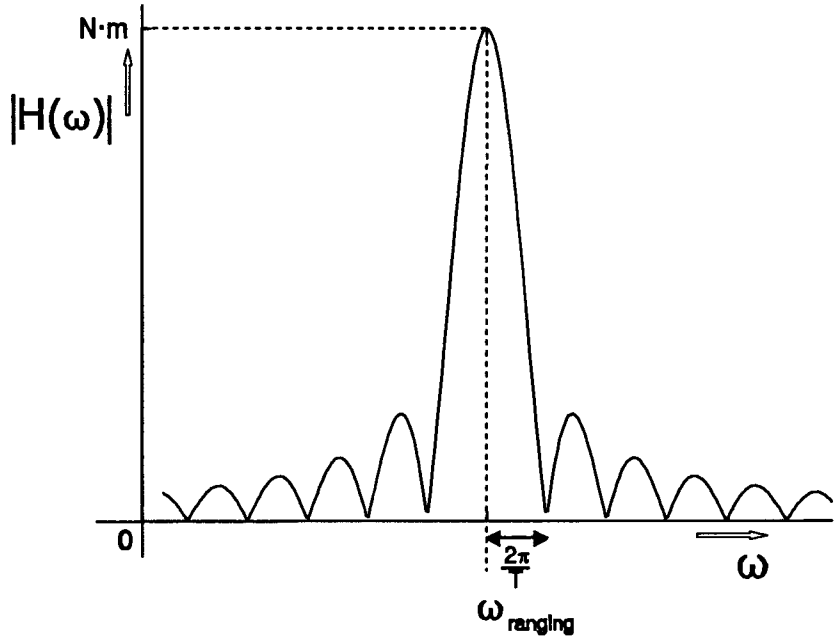

figure 6.2: The transfer function of the Discrete Fourier Transformation

To calculate the improvement of SNR, we need to know the Equivalent Noise BandWidth (ENBW) of the DFT. The ENBW can be calculated by:

$$B_N = \frac{1}{G_a}\int_{-f_s/2}^{f_s/2} |H(f)|^2\, df = \frac{1}{G_a}\int_{-f_s/2}^{f_s/2} \left|\frac{\sin(Nm\pi(f-f_{ran})T_s)}{\sin(\pi(f-f_{ran})T_s)}\right|^2 df \qquad (47)$$

where $G_a = |H(f)|^2_{max} = (T/\tau)^2 = (N\cdot m)^2$ is the maximum available power gain. This integral is evaluated by a numerical approximation. The ENBW can be approximated by:

$$B_N \approx \frac{1}{Nm}\cdot f_s = \frac{1}{m}\cdot f_{ranging} \qquad (48)$$

Now we have the equivalent noise bandwidth of the DFT and we know which higher harmonics will influence the phase measurement, so we can take a look at some DSP algorithms.

6.3 Digital signal processing software

In section 4.3 the used method for phase comparison is briefly described and in figure 4.6 is shown that the micro-processor besides the discrete Fourier transformation performs some filtering. This filtering is used to reduce the number of samples for the DFT part. As described in the previous section the DFT filters the input signal and if sufficient samples are used (increasing m), the ENBW becomes small enough to determine the ranging signal phase with the required accuracy. But using a large number of samples for the DFT will result in a large amount of required CPU-time, so if the signal is filtered before the DFT, then less samples are needed for the DFT.
In this section three algorithms are considered, first if 150 samples per ranging period for the DFT and no extra filtering is used, second if extra filtering and only 4 samples per ranging period for the DFT are used and third if extra filtering and 5 samples per ranging period for the DFT are used.

150 samples per ranging period for the DFT
Because no extra filtering is used, the DSP algorithm is very simple and shown in eq. 49.

$$\sum_{k=0}^{m\cdot N-1} x(k)\cdot e^{\frac{-j2\pi k}{N}} = \sum_k x(k)\cdot\cos\left(\frac{2\pi k}{N}\right) - j\sum_k x(k)\cdot\sin\left(\frac{2\pi k}{N}\right)$$

$$= a - j\cdot b \qquad (49)$$

$$\phi = atan\left(\frac{a}{b}\right)$$

In this situation the thermal noise and shot-noise descriptions and figures as given in the previous chapter are valid without any modification. Concerning the higher harmonics, the DFT uses 150 samples per ranging period, so N = 150 and the ranging signal is affected by the (1 + iN)th harmonics. When the power of these harmonics is calculated (section 5.2) and compared with the 1st harmonic (ranging signal), we see that their influence is negligible (more than 80 dB down).
A second aspect is the required CPU-time. To get any insight in the required CPU-time an estimation is made of the number of calculations, divided in additions and multiplications. The function ϕ = atan(a/b) is not considered, because it is the same in all implementations. From eq. 49, we obtain 2·m·N multiplications and 2·(m·N - 1) additions. But when we first add the samples, which must be multiplied by the same coefficient (x(k) + x(k+N) + x(k+2N) +..), the number of multiplications decreases to 2·N. Because these new samples are used with the sinus and cosines coefficients the number of additions is also reduced. First the new samples are calculated which costs (m-1)·N additions. Second the results after multiplication by the coefficients have to be added. This costs 2·(N-1) additions. So in total we have (m-1)N + 2(N-1) = N(m+1) - 2 = 150·m + 148 additions.

Four samples per ranging period for the DFT and extra filtering

The used micro-processor (68070) has a single instruction for additions (or subtractions) but has no single instruction for multiplications, so a multiplication takes much more time than an addition. To gain CPU-time we want to reduce the number of multiplications of the previous implementation. The DFT causes all the multiplications, thus if the number of samples used by the DFT is decreased, then the number of multiplications will decrease. When only four samples per ranging period are taken, the multiplication coefficients become: $\cos(0)=1$, $\cos(\pi/2)=0$, $\cos(\pi)=-1$, $\cos(3\pi/2)=0$, $\sin(0)=0$, $\sin(\pi/2)=1$, $\sin(\pi)=0$ and $\sin(3\pi/2)=-1$, in short only additions and subtractions are left.

Let us consider the consequences for aliasing. When we use four samples per ranging period (N=4) the ranging signal is disturbed by the (1+i·4)th harmonics, thus the 3rd, 5th, 7th, 9th, .. (all odd harmonics). At the same time the aliasing of the noise increases with a factor 150/4 with respect to the description given in section 5.1 (the total noise power remains the same, the noise bandwidth decreases and the noise density increases). This increase of aliasing can be reduced by filtering the samples before the discrete Fourier transform. If the signal bandwidth is smaller than 1/2 $f_{s,DFT}$ (≈½·40 kHz, half the sample frequency used by DFT), then no extra aliasing will occur. The applied filtering must be very simple, because the purpose of the filter is to decrease the number of multiplications and the required CPU-time. The averaging of a number of samples is such a simple filter and will be applied here. The transfer function of this filter is given in eq. 50 and shown in figure 6.3 and is equal to the transfer function of the DFT without the frequency shift [9].

$$H(e^{j\theta}) = \frac{\sin(L\cdot\frac{\theta}{2})}{\sin(\frac{\theta}{2})} \qquad (50)$$

where L is the length of the filter in number of samples and $\theta = \omega \cdot T_s$ is the normalized frequency.

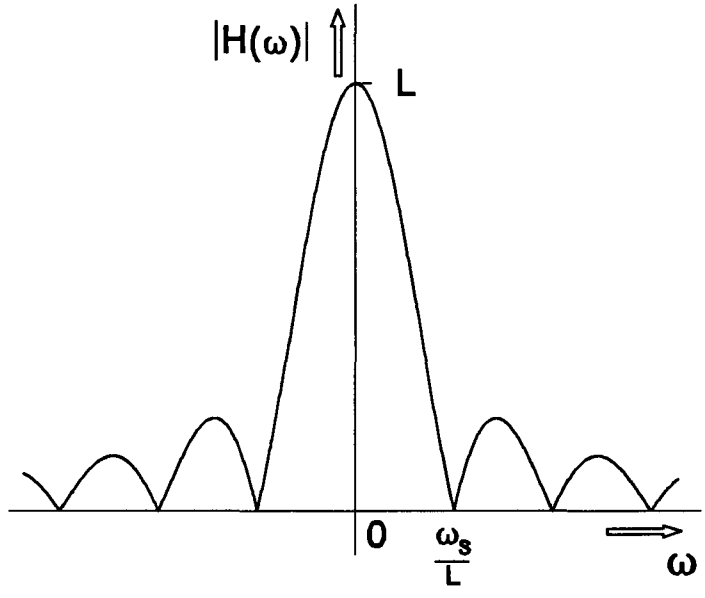

figure 6.3: The transfer function of the averaging filter

A very rough estimate of the filter bandwidth is given by:

$$B = \frac{1}{L} \cdot f_s \tag{51}$$

Substituting the bandwidth of 20 kHz in eq. 51 yields a filterlength L of approximately 70 samples.
By the averaging filter the noise density around the ranging frequency remains the same with respect to the ranging signal power and the higher harmonics are attenuated. Because of the filtering effect of the DFT the noise density around the ranging frequency is important for the accuracy and with respect to the previous implementation this is the same. The disadvantage of this implementation is the influence of the odd harmonics.
The DSP algorithm for this implementation is given by:

$$\begin{aligned}
x'(k) &= \sum_{s=0}^{m-1} x(k+sN) \qquad k = 0, 1, .., N-1 \\
x''(k) &= \sum_{l=kN/4}^{kN/4+L} x'(l) \qquad k = 0, 1, 2, 3 \\
&\sum_{k=0}^{3} x''(k) \cdot e^{\frac{-j2\pi k}{4}} = x''(0) - x''(2) - j(x''(1) - x''(3)) \\
\phi &= atan\left(\frac{x''(0) - x''(2)}{x''(1) - x''(3)}\right)
\end{aligned} \tag{52}$$

Again the samples shifted over a ranging period are added before the averaging filter is performed. This is done because if the length of the averaging filter (L) multiplied by the number of samples used for the DFT is larger than the number of samples per ranging period (N), then it is better to perform the filtering over the periods before the averaging filter. If the length of the averaging filter (L) multiplied by the number of samples used for the DFT is smaller than the number of samples per ranging period (N), then it is better to perform the averaging filter first.
From the first step is obtained N(m-1) = 150(m-1) additions (N samples over m periods), the next step results in 4(L-1) = 4(70-1) = 279 additions (the result of the averaging filter must be calculated for the 4 samples used by the DFT) and finally the last step results in 2 additions (x"(0)-x"(2) and x"(1)-x"(3)). Totally this algorithm has 150(m-1)+281 = 150·m +131 additions and no multiplications. This is an improvement of 300 multiplications and 17 additions with respect to the first algorithm.

Five samples per ranging period for the DFT and extra filtering

A disadvantage of the previous method is the influence of the odd harmonics. With five samples for the DFT the influence of higher harmonics can be made negligible and there still is an improvement of the required CPU-time.

As described in section 6.1 the ranging signal phase measurement is influenced by the (1+iN)th harmonics. When N is odd (e.g. 5) the result is mainly influenced by even harmonics. If the length of the filter is adjusted to a certain length, then the bandwidth is smaller than 1/2 $f_{s,DFT}$ (≈25 kHz) and the zero-crossings of the transfer function lie exactly on all even harmonics. Because the filter is in front of the DFT part, the phase measurement will not be affected by even harmonics. However the result is still affected with the 149th, 151th, 299th, 301th, .. harmonics, because this aliasing is caused by the first sampling. But as stated before these harmonics are negligible. If we want the zero-crossings of the transfer function correspond to the even harmonics, then with eq. 50 we find:

$$\sin\left(L \cdot \frac{2\pi \cdot 2nf_{ranging} \cdot T_s}{2}\right) = 0 \tag{53}$$

because,

$$T_s = \frac{1}{f_s} = \frac{1}{150 f_{ranging}} \tag{54}$$

we find:

$$L \cdot \frac{2\pi \cdot 2nf_{ranging}}{2 \cdot 150 f_{ranging}} = n\pi$$

$$L = \frac{150}{2} = 75 \tag{55}$$

Substituting L=75 in eq. 51 yields a bandwidth of B = 18 kHz, which is sufficient to maintain the noise density at the same level with respect to the ranging signal. The transfer function is shown in figure 6.4.

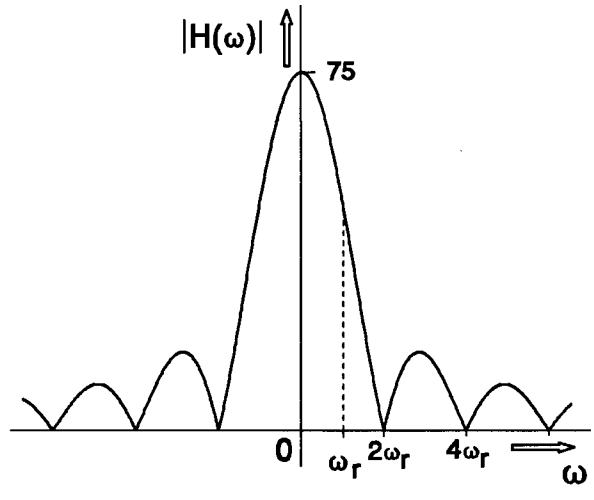

figure 6.4: The transfer function of the averaging filter with length 75

The DSP algorithm for this five points DFT is given by eq. 56.

$$x'(k) = \sum_{s=0}^{m-1} x(k+sN) \qquad k = 0, 1, .., N-1$$

$$x''(k) = \sum_{l=kN/5}^{kN/5+L} x'(l) \qquad k = 0, 1, 2, 3, 4$$

$$\sum_{k=0}^{4} x''(k) \cdot e^{\frac{-j2\pi k}{5}} = \sum_k x''(k) \cdot \cos\left(\frac{2\pi k}{5}\right) - j\sum_k x''(k) \cdot \sin\left(\frac{2\pi k}{5}\right) = a - jb \qquad (56)$$

$$\phi = atan\left(\frac{a}{b}\right)$$

The order of the first two steps is again determined by the length of the averaging filter and the number of samples used for the DFT.
In the first step we have N(m-1) = 150(m-1) additions, 5(L-1) = 5(75-1) = 370 additions in the second step and 2(5-1) = 8 additions and 2·5 = 10 multiplications in the third step. In total this yields 150(m-1)+378 = 150·m + 228 additions and 10 multiplications. Compared with the first implementation this yields an improvement of 290 multiplications and a loss of 80 additions.

The characteristics of the three implementations are summarized in table 6.1.

Table 6.1: Characteristics of three implementations

	# of multiplications	# of additions / subtractions	influence higher harmonics	extra aliasing
150 sampl./DFT	300	150m+148	negligible	No
4 samples/DFT filterlength 70	0	150m+131	yes (odd)	No
5 samples/DFT filterlength 75	10	150m+228	negligible	No

The algorithm with four samples per DFT is not used, because it is influenced by higher harmonics. The other two algorithms result in the same accuracy, but the five samples per DFT algorithm uses less CPU-time, so the algorithm with five samples per DFT and filtering will be implemented.

6.4 Estimation of inaccuracy

In chapter 3 is described that the Static Coarse Ranging is allowed to fail in 1% of the static coarse ranging procedures. The Static Coarse Ranging has failed when the measured delay differs from the real delay so much that the Static Fine Ranging preamble sent by the NU under ranging, does not fit in the idle time slot.

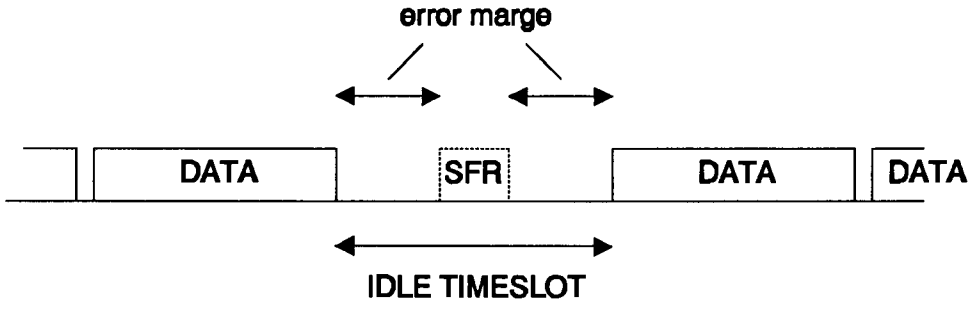

figure 6.5: Upstream traffic during the Static Fine Ranging

The length of a time slot is 56 bytes. Because a preamble is 3 bytes long the error marge at both sides is (56-3)/2 bytes. This means the Static Coarse Ranging procedure is allowed to have an inaccuracy of more than 212 bits in 1% of the occasions.
First the static errors are considered. The offset between LT-transmitter and LT-receiver slotclock has only influence on the measured absolute delay time (see section 5.2). The Static Coarse, the Static Fine and the Dynamic Fine Ranging are all related to the LT-receiver slotclock, hence the SFR preamble will not shift with respect to the data packets because of this offset. Next the component variations, as discussed in section 5.2 the maximum variation at the NT side has been specified at 12 ns, which corresponds to 7.5 bits. At the LT side the maximum variation has been specified at 6 ns, which corresponds to 3.7 bits. Totally the component variation causes an inaccuracy of 11.2 bits. The last static error is the non-linearity of the NT laser. This non-linearity could have an enormous influence, but as described in section 6.3 this influence has become negligible by the used DFT algorithm.
After subtraction of these static errors the error marge left for the dynamic errors is 212 - (11.2 / 2) = 206.4 bits.

Because the dynamic error sources are assumed to be gaussian distributed it is useful to express the required accuracy in a Signal-to-Noise Ratio (SNR). For the variance of the phase error we have [8]:

$$\overline{\Delta\theta_o^2} = \frac{N}{S} \qquad (57)$$

where $\Delta\theta_o$ is the phase error in radian.
The variance of the phase error, which corresponds to 1% failures can be determined with help of the gaussian distribution. First the phase error of 206 bits must be expressed in radian. One ranging period consists of 150 time slots and a time slot is 448 bits. These 150·448 = 67200 bits correspond to one ranging period, which is 2π rad.

An error of 206 bits is equal to:

$$\Delta\theta_{o,206} = \frac{206}{67200} \cdot 2\pi = 1.93 \cdot 10^{-2}\ rad \tag{58}$$

when 1% of the measurements has a phase error of more than $\Delta\theta_{o,206}$, we find with the gaussian distribution a standard deviation σ of:

$$\Delta\theta_{o,206} = k \cdot \sigma = 2.57 \cdot \sigma$$

$$\sigma = \frac{\Delta\theta_{o,206}}{k} = \frac{\Delta\theta_{o,206}}{2.57} = \frac{1.93 \cdot 10^{-2}}{2.57} = 7.5 \cdot 10^{-3}\ rad \tag{59}$$

This yields

$$\overline{\Delta\theta_o^2} = \sigma^2$$

$$= 5.62 \cdot 10^{-5}\ rad^2 \tag{60}$$

Substituting eq. 60 in eq. 57 results in

$$\frac{S}{N} = \frac{1}{5.62 \cdot 10^{-5}} = 1.78 \cdot 10^4$$

$$= 42.5\ dB \tag{61}$$

which is the required Signal-to-Noise ratio.

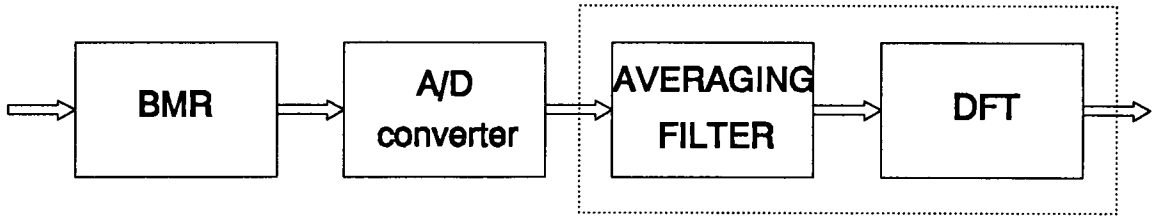

figure 6.6: The block diagram of the Static Coarse Ranging

In figure 6.6 the block diagram of the Static Coarse Ranging is shown and the ranging signal is fed to the Burst Mode Receiver. In the photodiode of the BMR thermal noise and shot-noise is added to the ranging signal. Considering the worst case ranging signal we find a thermal noise of -130.5 dBA^2 (eq. 15) and a shot-noise of -141.9 dBA^2 (eq. 19). The total noise power after the BMR becomes -130.2 dBA^2. The ranging signal power after the BMR is -120.0 dBA^2 and the noise density of the thermal and shot noise around the ranging frequency η is -191.6 dBA^2/Hz.
Next the signal is converted from analog to digital by the A/D converter. This A/D converter adds quantization noise. The quantization noise is maximum -163.9 dBA^2 and is negligible with respect to the thermal and shot noise.

In the micro-processor the averaging filter is performed. As shown in figure 6.4 and eq. 50 the transfer function of the averaging filter for the ranging frequency is:

$$|H(f_r)| = \left|\frac{\sin(75 \cdot 2\pi f_r \cdot \frac{T_s}{2})}{\sin(2\pi \cdot f_r \cdot \frac{T_s}{2})}\right| = \left|\frac{\sin(150\pi \cdot \frac{f_s}{150} \cdot \frac{1}{2f_s})}{\sin(2\pi \cdot \frac{f_s}{150} \cdot \frac{1}{2f_s})}\right| \tag{62}$$

$$= \left|\frac{\sin(\frac{\pi}{2})}{\sin(\frac{\pi}{150})}\right| = 47.75$$

The power of the ranging signal becomes:

$$\begin{aligned} S_o &= S_i \cdot |H(f_r)|^2 \\ &= -120\ dBA^2 + 33.6\ dB \\ &= -86.4\ dBA^2 \end{aligned} \tag{63}$$

The extra increase of the noise density for frequencies smaller than the ranging frequency can be exchanged with the diminished increase of the noise density for frequencies larger than the ranging frequency. So on an average the noise density around the ranging frequency also increases with 33.6 dB and η becomes -191.6 dBA^2/Hz + 33.6 dB = -158.0 dBA^2/Hz. This signal is fed to the Discrete Fourier Transformation. The equivalent noise bandwidth of the DFT filtering is given by eq. 48 and is f_r/m Hz. The total noise power after the DFT is given by:

$$\begin{aligned} N &= \eta \cdot B_N \\ &= -158.0\ dbA^2/Hz + 10 \cdot \log\left(\frac{f_r}{m}\right) dBHz \\ &= -158.0 + 39.7 - 10 \cdot \log(m)\ \ dBA^2 \\ &= -118.3 - 10 \cdot \log(m)\ dBA^2 \end{aligned} \tag{64}$$

Eq. 63 together with eq. 64 yields:

$$\frac{S}{N} = 31.9 + 10 \cdot \log(m)\ dB \tag{65}$$

Substituting eq. 65 in eq. 61 yields for m:

$$\begin{aligned} 31.9 + 10\cdot\log(m) &> 42.5 \\ 10\cdot\log(m) &> 10.6 \\ m &> 10^{1.06} = 11.5 \end{aligned} \tag{66}$$

To fulfill the requirements easily a measurement over 15 periods has been chosen. Substituting m = 15 in eq. 65 yields:

$$\frac{S}{N} = 31.9 + 11.8 = 43.7\ dB \tag{67}$$

hence,

$$\sigma = 6.56\cdot10^{-3}\ rad \tag{68}$$

with the maximum phase error, $\Delta\theta_{o,206}$, we find:

$$k = \frac{\Delta\theta_{o,206}}{\sigma} = 2.94 \tag{69}$$

and substituting k in the gaussian distribution yields an error rate of 0.30%, so the requirement of maximum 1% failures is fulfilled.

7. Description of the simulation model

In the previous chapters attention is paid to different concept choices, error sources and the accuracy. This has result in an estimation of the performance. To verify these results a simulation program has been developed (Appendix 1). This simulation program simulates the Static Coarse Ranging procedure. First the coarse ranging output signal of the burst mode receiver is simulated. This is the ranging signal together with thermal and shot noise. The signal-to-noise ratio of this signal is determined by the thermal and shot noise and the power of the received ranging signal. After this the A/D converter is simulated by quantizing the signal to the levels of the A/D converter. Next the filtering and DFT as described in section 6.3 is performed. This part of the software is identical to the part which will be implemented in the BAF network. Because we generate the input ranging signal, we know exactly the phase of this signal and it can be compared with the phase which has been calculated by the DFT part. If many of these simulations are performed, something can be said about the percentage of failures and the variance of the phase error (difference between input phase and calculated phase).
In section 7.1 the assumptions and parameters of the program are discussed and in section 7.2 the program structure is described. Finally in section 7.3 the simulation results are shown and compared with the performance estimation.

7.1 Assumptions and parameters

The simulation program has been based upon the diagram shown in figure 7.1 and the following assumptions have been made:

- no data interference during sampling
- maximum network attenuation upstream of 29.3 dB
- thermal noise in photodiode: bandwidth of 400 MHz, 15 pA/√Hz
- shot-noise is small with respect to thermal noise.

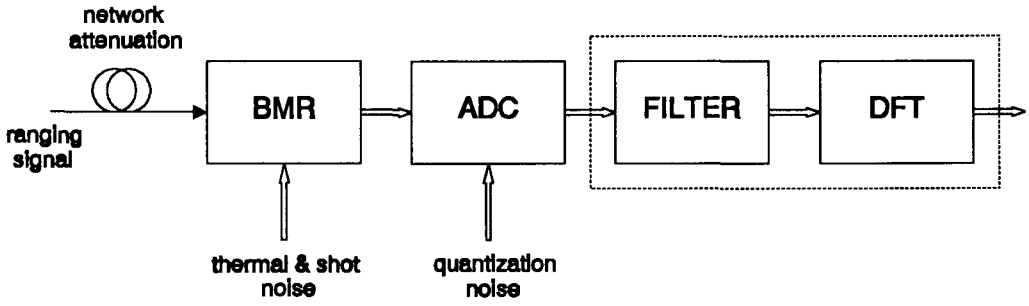

figure 7.1: Block diagram of Static Coarse Ranging

Because we want to do simulations for different configurations the program has parameters, which can be used to configure the system. These parameters are the number of samples per ranging period (N), the network attenuation, the resolution of the A/D converter, the length of the averaging filter (L), the number of used ranging periods (m) and the number of samples per ranging period used for the DFT. The program asks for this parameters before the simulation.

7.2 Program structure

The program simulates a number of phase measurements for the given system configuration and uses the pre-defined and measured phase to determine the phase error, the standard deviation of the phase error and the Signal-to-Noise Ratio. A special counter counts the phase errors which are larger than $1.93 \cdot 10^{-2}$ rad (=206 bits). The total number of simulated measurements can be changed.
The program has been written in C and has been compiled with the UNIX C compiler. The structure of the program is shown in figure 7.2.

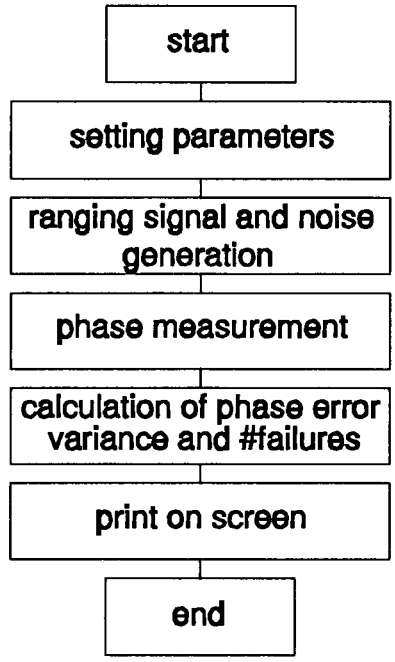

figure 7.2: The structure of the simulation program

First the program asks one by one the parameters and how many measurements must be used for the determination of the SNR (the more measurements the better the estimation). The next step is to generate the ranging signal added with noise. Therefor samples are taken of a sinus with pre-defined phase and a random gaussian distributed variable is added. From section 5.1 is obtained a minimal SNR after the sample and hold of 10.2 dB (S = -120.0 dBA^2, $N_{thermal\ \&\ shot}$ = -130.2 dBA^2). The signal power for a network attenuation of 29.3 dB (min. signal power) is upscaled from -120 dBA^2 to 0 dBA^2 in the simulation program. With the SNR of 10.2 dB this yields for the noise power in the simulation model:

$$N_{sim} = -10.2\ dBA^2 = 9.55 \cdot 10^{-2}\ A^2 \qquad (70)$$

we have

$$N = \sigma^2 \qquad (71)$$

hence, for the simulation model:

$$\sigma_{sim} = \sqrt{N_{sim}} = 3.09 \cdot 10^{-1}\ A \tag{72}$$

The noise which is added in the simulation model has a standard deviation of 0.309 A. The distribution of the used noise source is shown in Appendix 2 and is almost gaussian.

After generation of the samples (double precision) these are converted to quantized digital values with the given resolution as in the A/D converter (output is an integer).
The averaging filter uses these samples to calculate the new samples for the Discrete Fourier Transformation. The averaging filter and the DFT use an algorithm like the one described in eq. 56 (section 6.3). The measured phase is compared with the pre-defined phase and if the phase error is larger than $\Delta\theta_{0,206}$ then a counter is incremented. This counter counts the number of failures. To determine the variance of the phase error the formula given by eq. 73 is used.

$$\sigma^2 = \overline{\Delta\theta^2} - \overline{\Delta\theta}^2 \tag{73}$$

where $\Delta\theta$ is the phase error. After the simulated phase measurements, the SNR, the standard deviation, the percentage failures and the mean measured phase are written to the screen.
The input and output format of the program are shown in figure 7.3. For further information see Appendix 1.

INPUT:

Number of samples per ranging period (N): *150*
Network attenuation [dB] : *29.3*
Resolution of the ADC [in bits] : *12*
Length averaging filter (L): *75*
Number of used ranging periods (m): *15*
Number of samples used for DFT : *5*
How many measurements must be used : *20000*

OUTPUT:

percentage failures:	0.30 %
mean of phase error:	0.0000 rad
standard deviation:	6.5794e-03 rad
Signal-to-Noise Ratio:	43.6 dB

Do you want to quit? (yes=1, no=0) : *1*

figure 7.3: Input and output example of the simulation program

7.3 Simulation results

In this section the results of the simulation program are compared with the theoretical description of the Static Coarse Ranging method. The simulation program has been used to perform some simulations considering the performance of the Static Coarse Ranging. There have been run simulations for different values of m (the number of used ranging periods), different A/D converter resolutions, bottoming of the laser output and the influence of bottoming on a four points DFT. All simulations have used 20000 (simulated) measurements to determine the Signal-to-Noise Ratio, the variance of the phase error and the percentage failures.

First the Static Coarse Ranging performance as function of the number of used ranging periods is considered. The theoretical values are calculated with eq. 65, eq. 57, 58, 59, 60 and the gaussian distribution (Appendix 3). The results are shown in figure 7.4.

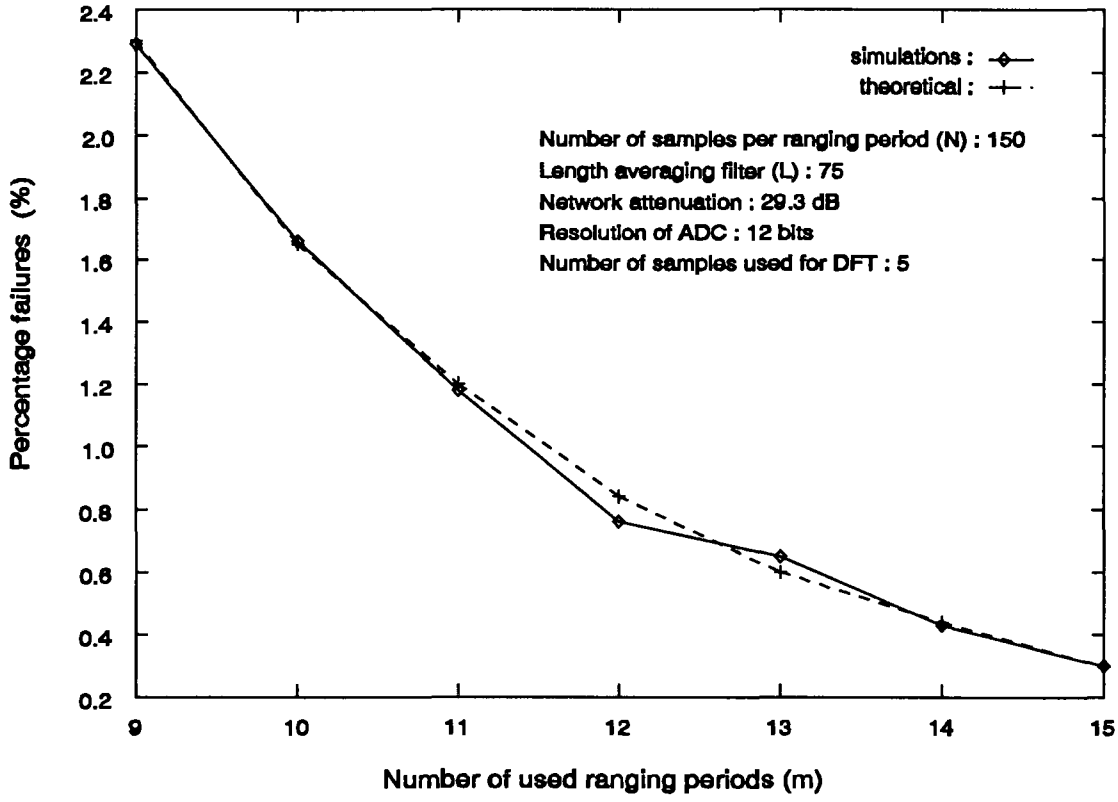

figure 7.4: Static Coarse Ranging failures vs. number of used ranging periods

Next the performance as function of the A/D converter resolution is depicted in figure 7.5. To calculate the theoretical values we use:

$$N_{tot} = N_{thermal} + N_{shot\text{-}noise} + N_{ADC} \tag{74}$$

We assume for the minimal upstream network attenuation (14.74 dB [2]) a maximum peak-peak amplitude of the ranging signal after the Burst Mode Receiver of 2 Volt. The maximum upstream network attenuation is 29.3 dB, so the minimum peak-peak amplitude

of the ranging signal after the Burst Mode Receiver is 2 V / $10^{(2.93-1.47)}$ = 70.0 mV. The input range of the A/D converter is 2 V and with b bits the resolution is given by:

$$\frac{2V}{2^b} = 2^{-b+1}\ V/LSB \tag{75}$$

The number of steps used by the ADC for the minimum ranging signal is:

$$n = \frac{70.0 \cdot 10^{-3}}{2^{-b+1}}\ LSB \tag{76}$$

Substituting this and the minimum signal power (eq. 7) in eq. 22 yields the quantization noise power added by the A/D converter (N_{ADC}).
The change in N_{tot} must be corrected in eq. 65 and further with eq. 57, 58, 59, 60 and the gaussian distribution we find the theoretical values.

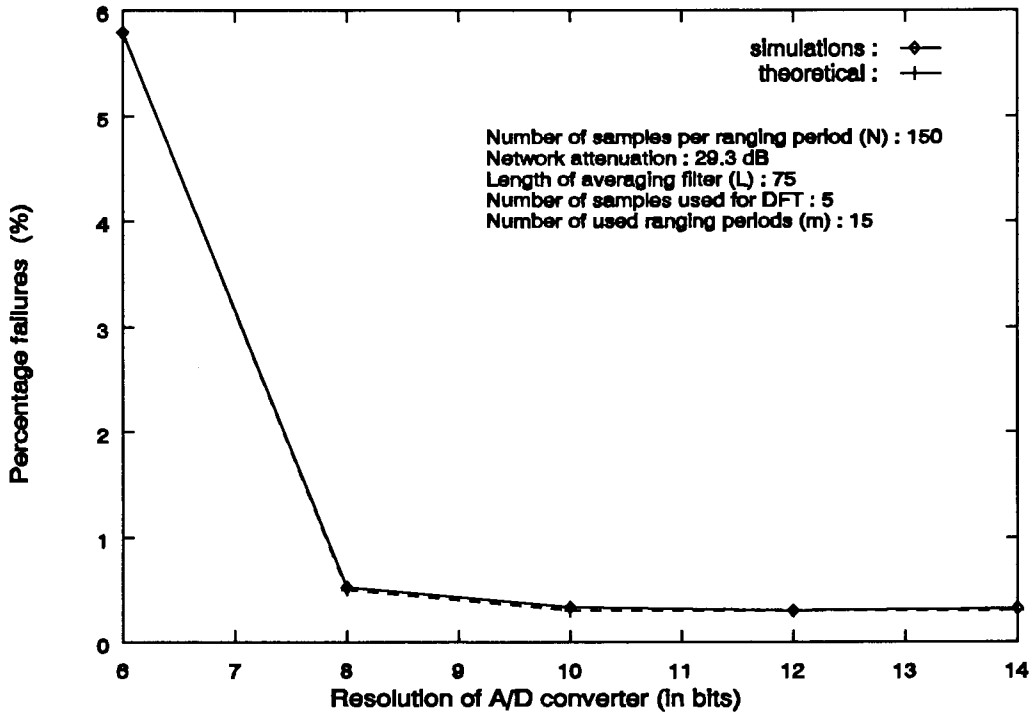

figure 7.5: Static Coarse Ranging failures vs. ADC resolution

Third bottoming of the laser output signal is considered. As described in chapter 6 bottoming causes higher harmonics, but the used algorithm filters these higher harmonics before the phase measurement. However the power of the first harmonic (the ranging signal) decreases, when bottoming of the laser output signal occurs. This yields a decrease of the Signal-to-Noise Ratio. The power of the first harmonic with respect to the power of the first harmonic when no bottoming occurs (x = 1) can be calculated with eq. 38. The change in signal power can be expressed as:

$$\Delta S_{ranging} = 20 \cdot \log\left(\frac{b_{1,x}}{b_{1,x=1}}\right) dB \tag{77}$$

The theoretical values can be calculated with eq. 65 corrected by eq. 77, eq. 57 - 60 and the gaussian distribution. For the simulation of this input signal the simulation program must be modified and the sinus samples are limited at the bottomside. The results of the simulations are given in figure 7.6.

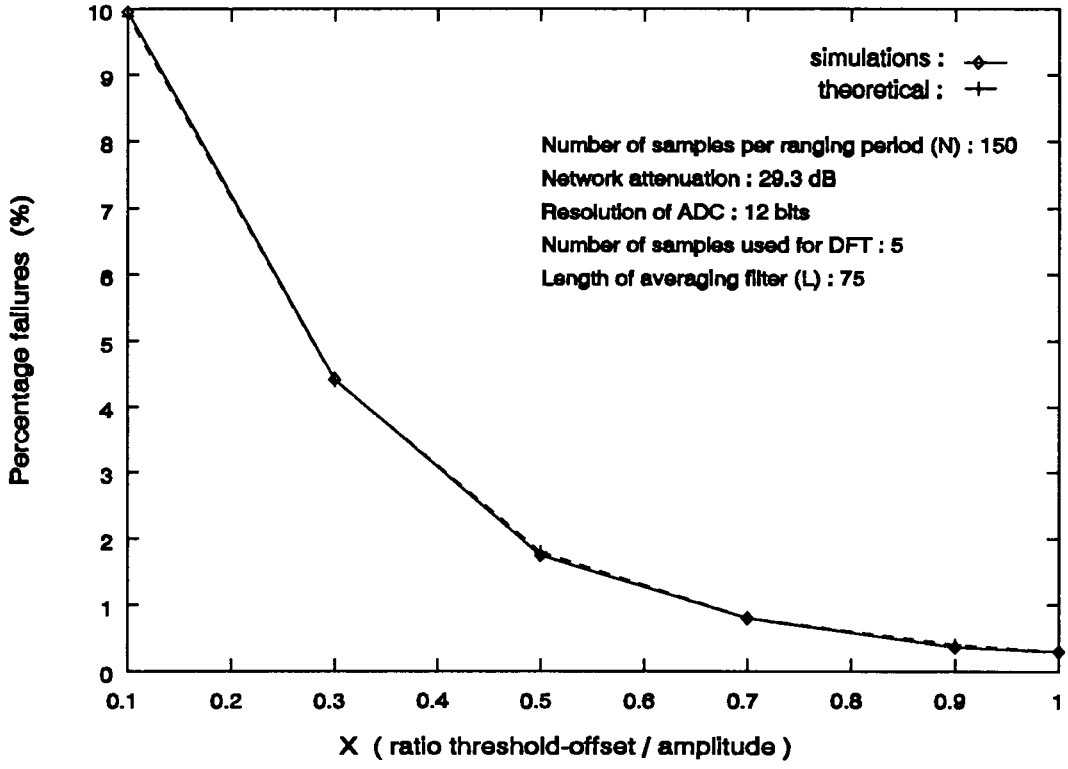

figure 7.6: Static Coarse Ranging failures vs. bottoming of the laser output signal

Looking at figure 7.4, 7.5 and 7.6 we see a close agreement between the theoretical values and the simulation results. So the assumptions and calculations concerning the noise influence are justified.

Finally a simulation has been performed which uses four samples per DFT and with bottoming of the laser output signal.

X = 0.5	4-pts	5-pts
percentage failures:	21.24 %	1.75 %
mean of phase error:	0.0126 rad	-0.0001 rad
standard deviation:	8.3718e-03 rad	8.2072e-03 rad
Signal-to-Noise Ratio:	41.5 dB	41.7 dB

figure 7.7: Simulation results of 4- and 5-points DFT

The result of this simulation given by figure 7.7, shows that the variance of the phase error (and the SNR) remains the same, but the mean value of the phase error is not zero. This means that the phase measurement is influenced by the higher harmonics and this influence can be seen as a static error.

8. Conclusions and recommendations

In this report a new method has been described to determine the transfer delay between a Network Unit and a Line Termination of a broadband access facilities network. The method, which uses a low frequency, low level signal, is the first step of totally three steps to put all Network Units at the same virtual distance. This first step is called Static Coarse Ranging. The low frequency, low level ranging signal is superimposed on the upstream data traffic by a Network Unit and at the Line Termination the phase of the received ranging signal is determined. The detection of the ranging signal in the LT is done by sampling in the gap between adjacent BAF-cells. The phase determination of the ranging signal is realized by a software algorithm which uses Discrete Fourier Transformation techniques. The advantages and disadvantages of the described method are given in table 8.1.

Table 8.1: Advantages/disadvantages of the DFT based Static Coarse Ranging method

Advantages	Disadvantages
data traffic not interrupted	extra amount 'dc'-light (9.3kHz) received by the Burst Mode Receiver
can be used for other purposes	
no influence of data traffic	required CPU-time to calculate the transfer delay
negligible influence of higher harmonics	
high precision	

A description and measurement of the higher harmonics caused by bottoming of the laser is given in section 5.2. The description gives a good approximation of the maximum distortion of the laser module output in the measurement setup.
In section 6.4 an estimation of the inaccuracy of the proposed Static Coarse Ranging has been made. To verify the calculated performance of the Static Coarse Ranging the simulation program SIM has been developed. There has been found a close agreement between the simulation results and the calculated performance.
The proposed Static Coarse Ranging method with an A/D converter of 12 bits, a measurement over 15 periods, an averaging filter with a length of 75 samples and 5 samples used for the DFT fulfills the requirements and in worst case 0.30 % of the Static Coarse Ranging procedures fails.
To improve the accuracy of the Static Coarse Ranging the number of periods which is used for a phase measurement must be increased. The required time for Static Coarse Ranging also will increase. First because more samples have to be taken and second because the number of calculations increases.
The maximum feasible accuracy is determined by the static error sources and in our case this is 11.2 bits.

When the proposed Static Coarse Ranging is implemented special attention must be paid to the static errors in the NU and the LT because they always affect the Static Coarse Ranging result. Also attention must be paid to the Static Coarse Ranging software, so that the required CPU-time is minimized.

Because DFT techniques are used to determine the phase of the ranging signal, it is very simple to determine also the amplitude of the ranging signal. This extra information can be used to establish the status of the delay measurement, meaningful or not meaningful. Also this information can be used for other purposes like fibre monitoring and polling, so it is useful to implement this amplitude measurement.
When this amplitude measurement is implemented, perhaps it is useful to determine the phase over e.g. 8 periods and with help of the amplitude measurement to decide or it is necessary to use the next e.g. 7 periods. In most of the situations the network attenuation is much less than 29.3 dB and a measurement over 8 periods is sufficient to meet the requirements by this a reduction of the required measurement- and CPU-time is achieved.

References

[1] Mosch, T.W.M.
Ranging method using low level/low frequency signal
AT&T Network Systems Nederland, Huizen: department Explorations, 1992
int. ref. JNL210-R-5100-92217

[2] Low Level Specification of the Access Facilities, BAF Deliverable 5, RACE 2024
Ed. by Cray Communications: M. Shaw and D. Patel
Watford (UK) : Cray Communications, 1992
reference: R2024_CRA_W31_DS_I_005_b1

[3] Etten, W. van and J. van der Plaats
Fundamentals of optical fiber communications
London: Prentice Hall, 1991

[4] Carlson, A.B.
Communication systems, an introduction to signal and noise in electrical communication, 3rd ed.
Singapore: McGraw-Hill

[5] Verhoef, W.
Overall timing on the U-board
AT&T Network Systems Nederland, Huizen: department Explorations, 1993
int. ref. JNL210-R-5100-93084

[6] Oppenheim A.V. and R.W. Schafer
Theory and applications of digital signal processing
Englewood Cliffs, New York: Prentice-Hall, 1975 (p. 26-28)

[7] Enden, A.W.M. van den and N.A.M. Verhoeckx
Digitale signaalbewerking, 1st ed.
Amerongen (NL): Delta Press, 1987

[8] Gardner, F.M.
Phaselock Techniques
New York: Wiley, 1979

List of abbreviations

APD : Avalanche Photo Diode
ATM : Asynchronous Transfer Mode
BAF : Broadband Access Facilities
BMR : Burst Mode Receiver
DFT : Discrete Fourier Transformation
ENBW : Equivalent Noise Bandwidth
FTTC : Fibre To The Curb
FTTH : Fibre To The Home
HDWDM : High Density Wavelength Division Multiplexing
LEX : Local Exchange
LSB : Least Significant Bit
LT : Line Termination
MAC : Medium Access Control
NU : Network Unit
NT : Network Termination
OAM : Operation And Maintenance
PON : Passive Optical Network
RACE : Research and development in Advanced Communications technology in Europe
SNR : Signal-to-Noise Ratio
STM : Synchronous Transfer Mode
TDMA : Time Division Multiple Access
WDM : Wavelength Division Multiplexing

Appendix 1: Simulation program SIM


```
/*************************************************************/
/*                                                           */
/* SIM                                                       */
/*                                                           */
/* A Simulation Program for Static Coarse Ranging in the     */
/* BAF-LT. The ranging method uses DFT techniques to         */
/* determine the phase delay of the low level/low frequency  */
/* ranging signal superimposed on the upstream data traffic. */
/* A FIR filter precedes the DFT.                            */
/*                                                           */
/* Source ........ sim.c                                     */
/* Language ...... UNIX C++ compiler                         */
/* Date .......... 20-June-1993                              */
/* Written by .... A. van Oyen                               */
/*                 AT&T Network Systems Nederland BV         */
/*************************************************************/


/*************************************************************/
/* include files                                             */
/*************************************************************/
#include <stdio.h>
#include <math.h>
#include <stdlib.h>


/*************************************************************/
/* global definitions                                        */
/*************************************************************/
#define PI      3.14159265358979323846
#define NMAX    150
#define ADCMAX  81
#define PH0     0.0
#define LIMIT   0.019261
#define ABS(x)  (x<0 ? -x : x)


/*************************************************************/
/* function definitions                                      */
/*************************************************************/
int    ADC(double x,int n);
float  gasdev(int *idum);
float  ran1(int *idum);


/*************************************************************/
/* main function of SIM                                      */
/*************************************************************/
int main(void)
{
 double Re,Im,phase;
 double sigma[1000*NMAX],A,hulp,delta;
 double mean,msqr,variance,stdv,snr,attenuation;
 int    amet,h,i,j,b,N,n,m,stoppen,sample[1000*NMAX],L;
 int    dft,tail;


 h=1;
 stoppen=0;



 while(stoppen==0)
 {
  printf("\nNumber of samples per ranging period (N): ");
```

```
scanf("%d",&N);
printf("Network attenuation [dB] : ");
scanf("%lf",&attenuation);
printf("Resolution of the ADC [in bits] : ");
scanf("%d",&n);                                    /*************************/
printf("length averaging filter (L): ");           /* setting of parameters */
scanf("%d",&L);                                    /*************************/
printf("Number of used ranging periods (m): ");
scanf("%d",&m);
printf("Number of samples used for DFT : ");
scanf("%d",&dft);
printf("How many measurements must be used : ");
scanf("%d",&amet);


mean=0;
msqr=0;                                            /*************************/
A=sqrt(2)*pow(10,2.93-(attenuation/10));           /* initalization         */
tail=0;                                            /*************************/


for(b=0;b<amet;b++)
{

 Re=0;
 Im=0;

 for(i=0;i<m*N+L;i++)                              /*************************/
  {                                                /* clean up old samples  */
   sample[i]=0;                                    /*************************/
   sigma[i]=0.0;
  }


 for(i=0;i<m*N+L;i++)                              /*************************/
  {                                                /* generate samples of   */
   hulp=A*(sin(2*PI*i/N+PH0)+1)+0.309*gasdev(&h);  /* ranging signal and    */
   sample[i]=ADC(hulp,n);                          /* noise for one phase-  */
  }                                                /* measurement           */
                                                   /*************************/

 for(i=0;i<N;i++)                                  /*************************/
      {                                            /* summation of samples  */
       for(j=1;j<m;j++)                            /* x(k)+x(k+N)+x(k+2N)...*/
              {                                    /*************************/
               sample[i]+=sample[i+j*N];
              }

      }

 for(i=0;i<dft;i++)                                /*************************/
      {                                            /* averaging filter of   */
       for(j=i*N/dft;j<i*N/dft+L;j++)              /* length L              */
             {                                     /*************************/
              if (j>=N)
                      sigma[i]+=sample[j-N];
              else
                      sigma[i]+=sample[j];
             }
      }


 for(i=0;i<dft;i++)                                /*************************/
      {                                            /* Discrete Fourier      */
       Re+=sigma[i]*cos(2*PI*i/dft);               /* Transformation with   */
       Im+=sigma[i]*sin(2*PI*i/dft);               /* (dft) points          */
```

```
        }                                                   /*************************/

    phase=atan2(Re,Im) - PI*(L-1)/N;                        /*************************/
    if (phase< -PI)                                         /* phase calculation,    */
         phase+=2*PI;                                       /* last term is caused   */
                                                            /* by averaging filter   */
    delta=ABS((PH0-phase));                                 /*************************/
    if (delta>PI)
         delta=ABS((delta-2*PI));
    if (delta>LIMIT)                                        /*************************/
         ++tail;                                            /* calculation of phase  */
                                                            /* error and variance    */
    mean+=phase-PH0;                                        /*************************/
    msqr+=((phase-PH0)*(phase-PH0));

   )/*for b*/


   printf("\npercentage failures:        %4.2f %%",(float)100*tail/amet);
   mean=mean/amet;
   msqr=msqr/amet;                                          /*************************/
   variance=msqr - mean*mean;                               /* write results to the  */
   stdv=sqrt(variance);                                     /* screen                */
   snr=-10*log10(variance);                                 /*************************/
   printf("\nmean of phase error:       %5.4lf rad",mean);
   printf("\nstandard deviation:         %5.4le rad",stdv);
   printf("\nSignal-to-Noise Ratio:      %3.1lf dB\n",snr);

   printf("\nDo you want to quit? (yes=1,no=0) : ");
   scanf("%d",&stoppen);

  )/*while*/


  return(0);                                                /* end                   */

)/*main*/
```

```
/*************************************************************/
/* int ADC(double x, int n)                                  */
/*                                                           */
/* simulation of AD converter                                */
/* x is the input signal, n is the resolution of the ADC in  */
/* bits, return value is output value ADC                    */
/*************************************************************/
int ADC(double x, int n)
{
 int y;

 y=0x1<<n;          /* y=2^n */
 y=(int) floor ((y*x/ADCMAX)+0.5);
 if (y>=(0x1<<n))
        y=(0x1<<n)-1;
 if (y<0)
        y=0;

 return(y);
}
```

```
/*************************************************************/
/* float gasdev(int idum)                                    */
/*                                                           */
/* normally distributed deviate with zero mean and unit      */
/* variance                                                  */
/* SOURCE: "NUMERICAL RECIPES in C", W.H. Press,B.P. Flannery*/
/*         S.A. Teukolsky, W.T. Vetterling                   */
/*************************************************************/
float gasdev(int *idum)
{
        static int iset=0;
        static float gset;
        float fac,r,v1,v2;

        if  (iset == 0) {
                do {
                        v1=2.0*ran1(idum)-1.0;
                        v2=2.0*ran1(idum)-1.0;
                        r=v1*v1+v2*v2;
                } while (r >= 1.0 || r == 0.0);
                fac=sqrt(-2.0*log(r)/r);
                gset=v1*fac;
                iset=1;
                return v2*fac;
        } else {
                iset=0;
                return gset;
        }
}




/*************************************************************/
/* ran1()                                                    */
/*                                                           */
/* generates uniform distributed numbers between 0.0 and 1.0 */
/* SOURCE: "NUMERICAL RECIPES in C", W.H. Press,B.P. Flannery*/
/*         S.A. Teukolsky, W.T. Vetterling                   */
/*************************************************************/
#define M1 259200
#define IA1 7141
#define IC1 54773
#define RM1 (1.0/M1)
#define M2 134456
#define IA2 8121
#define IC2 28411
#define RM2 (1.0/M2)
#define M3 243000
#define IA3 4561
#define IC3 51349

float ran1(int *idum)
{
        static long ix1,ix2,ix3;
        static float r[98];
        float temp;
        static int iff=0;
        int j;
```

Resolution of the ADC: 6 bits
percentage failures: 5.79 %
mean of phase error: -0.0002 rad
standard deviation: 1.0180e-02 rad
Signal-to-Noise Ratio: 39.8 dB

Resolution of the ADC: 8 bits
percentage failures: 0.52 %
mean of phase error: -0.0000 rad
standard deviation: 6.9146e-03 rad
Signal-to-Noise Ratio: 43.2 dB

Resolution of the ADC: 10
percentage failures: 0.33 %
mean of phase error: 0.0001 rad
standard deviation: 6.6039e-03 rad
Signal-to-Noise Ratio: 43.6 dB

Resolution of the ADC: 12
percentage failures: 0.30 %
mean of phase error: -0.0000 rad
standard deviation: 6.5794e-03 rad
Signal-to-Noise Ratio: 43.6 dB

Resolution of the ADC: 14
percentage failures: 0.32 %
mean of phase error: -0.0000 rad
standard deviation: 6.5971e-03 rad
Signal-to-Noise Ratio: 43.6 dB

Simulation 3: failures vs. bottoming laser

Number of samples per ranging period (N): 150
Network attenuation: 29.3 dB
Resolution of the ADC: 12 bits
Length of averaging filter (L): 75
Number of used ranging periods (m): 15
Number of samples used for DFT: 5
How many measurement must be used: 20000

X = 1 (no bottoming)
percentage failures: 0.30 %
mean of phase error: -0.0000 rad
standard deviation: 6.5794e-03 rad
Signal-to-Noise Ratio: 43.6 dB

X = 0.9
percentage failures: 0.36 %
mean of phase error: 0.0000 rad
standard deviation: 6.7165e-03 rad
Signal-to-Noise Ratio: 43.5 dB

X = 0.7
percentage failures: 0.80 %
mean of phase error: 0.0001 rad
standard deviation: 7.2500e-03 rad
Signal-to-Noise Ratio: 42.8 dB

X = 0.5
percentage failures: 1.75 %
mean of phase error: -0.0001 rad
standard deviation: 8.2072e-03 rad
Signal-to-Noise Ratio: 41.7 dB

X = 0.3
percentage failures: 4.42 %
mean of phase error: 0.0001 rad
standard deviation: 9.5936e-03 rad
Signal-to-Noise Ratio: 40.4 dB

X = 0.1
percentage failures: 9.95 %
mean of phase error: 0.0002 rad
standard deviation: 1.1691e-02 rad
Signal-to-Noise Ratio: 38.6 dB

The results of simulation 4 (4 pts-DFT) are given in fig. 7.7 (page 45).

Appendix 5: Data sheet FU-44SLD-1

FU-44SLD-1

1.3 μm LD Module with Singlemode Fiber Pigtail

Module type FU-44SLD-1 has been developed for coupling a singlemode optical fiber and a 1.3μm wavelength InGaAsP LD (Laser diode).The package is incorporated with dual-in-line pins for electrical connection.

This module is suitable to light source for use in high-speed long haul digital optical communication systems and use in measuring instruments.

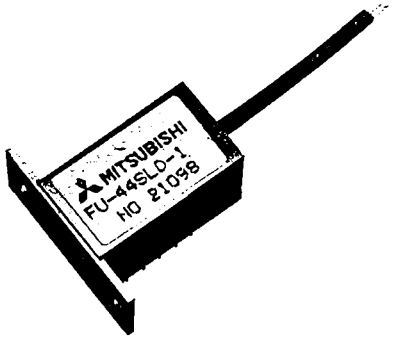

FU-44SLD-1

FEATURES

- High-speed response
- Emission wavelength is in 1.3μm band
- Low threshold current (10mA typ.)
- Built-in thermal electric cooler
- Dual-in-line package
- With photodiode for optical output monitor
- Diodes are hermetically sealed

ABSOLUTE MAXIMUM RATINGS (T_{LD}=25℃)

Items		Symbols	Conditions	Ratings	Units
Laser diode	Optical output power from fiber end	P_F	CW	3	mW
			Pulse (Note 1)	6	
	Reverse Voltage	V_{RL}	–	2	V
Photodiode for monitoring	Reverse Voltage	V_{RD}	–	15	V
	Forward Current	I_{FD}	–	2	mA
Operating case temperature		Tc	–	– 20~65	℃
Storage temperature		T_{stg}	–	– 40~70	℃

Note 1) Pulse condition : Pulse width ≤ 1μs, Duty ratio ≤ 50%

OUTLINE DRAWINGS Unit (mm)

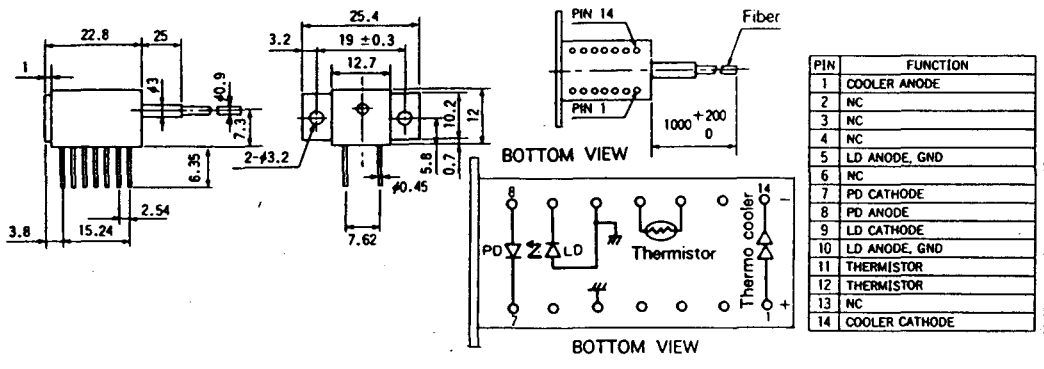

PIN	FUNCTION
1	COOLER ANODE
2	NC
3	NC
4	NC
5	LD ANODE, GND
6	NC
7	PD CATHODE
8	PD ANODE
9	LD CATHODE
10	LD ANODE, GND
11	THERMISTOR
12	THERMISTOR
13	NC
14	COOLER CATHODE

FU-44SLD-1

FU-44SLD-1

1.3 μm LD Module with Singlemode Fiber Pigtail

CHARACTERISTICS (T_C=25 °C, T_{LD}=25 °C, unless otherwise noted)

Items	Symbols	Conditions	Min.	Typ.	Max.	Units
Threshold current	I_{th}	CW	–	10	30	mA
Operating current	I_{op}	CW	–	25	45	mA
Operating voltage	V_{op}	CW, $I_F = I_{op}$ (Note 1)	–	1.2	1.6	V
Optical output power from fiber end	P_F	CW, $I_F = I_{op}$	1	2	–	mW
Central wavelength	λ_C	CW, $I_F = I_{op}$	1270	1300	1330	nm
Spectral bandwidth (RMS) (Note 3)	$\Delta\lambda$	CW, $I_F = I_{op}$	–	1.4	–	nm
Rise and fall times	t_r, t_f	$I_B = I_{th}$, 10~90 % (Note 2)	–	0.3	–	ns
Tracking error (Note 4)	E_r	T_C = – 20~65 °C, APC, ATC	–	0.2	–	dB
Differential efficiency	η	–	–	0.13	–	mW/mA
Monitor current	I_{mon}	CW, $I_F = I_{op}$, V_{RD} = 5V	0.1	0.6	–	mA
Dark current (Photodiode)	I_D	V_{RD} = 5V	–	0.1	1	μA
Capacitance (Photodiode)	C_t	V_{RD} = 5V, f = 1MHz	–	10	–	pF

Note 1) I_F : Forward current (LD)
Note 2) I_B : Bias current (LD)

Note 3) $$\Delta\lambda = \sqrt{\frac{\Sigma ai\,(\lambda i - \lambda c)^2}{\Sigma ai}} \quad (ai \geq ap \times 0.01)$$

ai : Relative intensity of laser spectral emission modes
ap : Peak of laser spectral emission modes

Note 4) $$E_r = MAX\left|10 \cdot \log \frac{P_F}{P_F\,(25℃)}\right|$$

THERMAL CHARACTERISTICS (T_{LD}=25 °C T_C= – 20°C~65°C)

Items	Symbols	Conditions	Min.	Typ.	Max.	Units
Thermistor resistance	R_{th}	T_{LD} = 25 °C	9.5	10	10.5	kΩ
B constant of thermistor resistance	B	–	–	3250	–	K
Cooling capacity	ΔT	T_C = 65 °C	40	–	–	°C
Cooler current	I_{pe}	ΔT = 40 °C	–	0.6	1	A
Cooler voltage	V_{pe}	ΔT = 40 °C	–	1.6	2	V

FIBER PIGTAIL SPECIFICATIONS

Items	Specifications	Units
Type	SM	–
Mode field dia.	10 ± 1	μm
Cladding dia.	125 ± 2	μm
Jacket dia.	0.9	mm

EXAMPLE OF CHARACTERISTICS

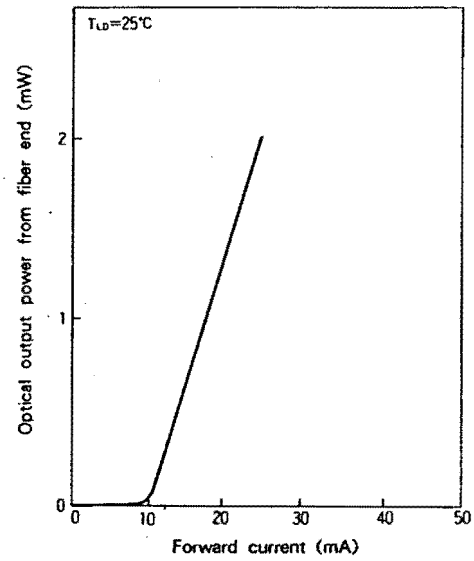

Forward current vs. Optical output power

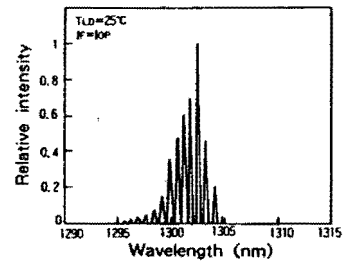

Light-emission spectrum

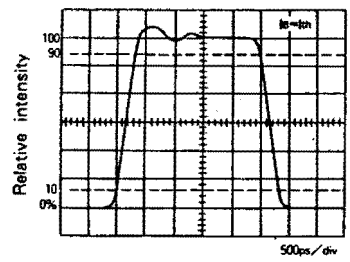

Pulse response

BAF, Broadband Access Facilities
AT&T-NS-NL, P.O.Box 18, 1270AA Huizen, Tel +3135874774, Fax +3135875954